

1 **Exploring the impacts of unprecedented climate extremes on forest ecosystems: hypotheses**
2 **to guide modeling and experimental studies**

3

4 Jennifer A. Holm^{1,*}, David M. Medvigy², Benjamin Smith^{3,4}, Jeffrey S. Dukes⁵, Claus Beier⁶,
5 Mikhail Mishurov³, Xiangtao Xu⁷, Jeremy W. Lichstein⁸, Craig D. Allen⁹, Klaus S. Larsen⁶, Yiqi
6 Luo¹⁰, Cari Ficken¹¹, William T. Pockman¹², William R.L. Anderegg¹³, and Anja Rammig¹⁴

7

8 ¹ Lawrence Berkeley National Laboratory, Berkeley, California, USA

9 ² University of Notre Dame, Notre Dame, Indiana, USA

10 ³ Dept of Physical Geography and Ecosystem Science, Lund University, Lund, Sweden

11 ⁴ Hawkesbury Institute for the Environment, Western Sydney University, Penrith, NSW 2751,
12 Australia

13 ⁵ Department of Forestry and Natural Resources and Biological Sciences, Purdue University,
14 West Lafayette, Indiana, USA

15 ⁶ Department of Geosciences and Natural Resource Management, University of Copenhagen,
16 Frederiksberg, Denmark

17 ⁷ Department of Ecology and Evolutionary Biology, Cornell University, Ithaca, New York, USA

18 ⁸ Department of Biology, University of Florida, Gainesville, Florida, USA

19 ⁹ U.S. Geological Survey, Fort Collins Science Center, New Mexico Landscapes Field Station,
20 Los Alamos, New Mexico, USA

21 ¹⁰ Center for Ecosystem Science and Society, Department of Biological Sciences, Northern
22 Arizona University, Flagstaff, Arizona, USA

23 ¹¹ Department of Biology, University of Waterloo, Waterloo, Ontario, Canada

24 ¹² Department of Biology, University of New Mexico, Albuquerque, New Mexico, USA

25 ¹³ School of Biological Sciences, University of Utah, Salt Lake City, Utah, USA

26 ¹⁴ Technical University of Munich, TUM School of Life Sciences Weihenstephan, Freising,
27 Germany

28

29 * *Correspondence to:* Jennifer Holm; 510-495-8083; jaholm@lbl.gov

30

31 **Keywords:** demographic modeling; mortality; drought; recovery; carbon cycle; nonstructural
32 carbohydrate storage; plant hydraulics; dynamic vegetation

33

34 **Abstract**

35

36 Climatic extreme events are expected to occur more frequently in the future, increasing the
37 likelihood of unprecedented climate extremes (UCEs), or record-breaking events. UCEs, such as
38 extreme heatwaves and droughts, substantially affect ecosystem stability and carbon cycling by
39 increasing plant mortality and delaying ecosystem recovery. Quantitative knowledge of such
40 effects is limited due to the paucity of experiments focusing on extreme climatic events beyond
41 the range of historical experience. Here, we present a road map of how dynamic vegetation
42 demographic models (VDMs) can be used to investigate hypotheses surrounding ecosystem
43 responses to one type of UCE: unprecedented droughts. As a result of nonlinear ecosystem
44 responses to UCEs, that are qualitatively different from responses to milder extremes, we
45 consider both biomass loss and recovery rates over time, by reporting a time-integrated carbon
46 loss as a result of UCE, relative to the absence of drought. Additionally, we explore how
47 unprecedented droughts in combination with increasing atmospheric CO₂ and/or temperature
48 may affect ecosystem stability and carbon cycling. We explored these questions using
49 simulations of pre-drought and post-drought conditions at well-studied forest sites, using equally
50 well-tested models (ED2 and LPJ-GUESS). The severity and patterns in biomass losses differed
51 sustainably between models. For example, biomass loss could be sensitive to either drought
52 duration or drought intensity depending on the model approach. This is due to the models having
53 different, but also plausible representations of processes and interactions, highlighting the
54 complicated interactions and variability of UCE impacts still needed to be narrowed down in
55 models. Elevated atmospheric CO₂ concentrations (eCO₂) alone did not completely buffer the
56 ecosystems from carbon losses during UCEs in the majority of our simulations. Our findings
57 highlight contrasting differences in process formulations and uncertainties in models, most
58 notably related to availability in plant carbohydrate storage and the diversity of plant hydraulic
59 schemes, in projecting potential ecosystem responses to UCEs. We provide a summary of the
60 current state and role of many model processes that give way to different underlying hypotheses
61 of plant responses to UCEs, reflecting knowledge gaps, which in future studies could be tested
62 with targeted field experiments and an iterative modeling-experimental conceptual framework.

63 **1 Introduction**

64 The increase in extreme climate and weather events, such as prolonged heatwaves and
65 droughts as seen over the last three decades, are expected to continue to increase in frequency
66 and magnitude, leading to progressively longer and warmer droughts on land (IPCC 2012, 2021).
67 Droughts are affecting all areas of the globe, more than any other natural disturbance, and recent
68 droughts have broken long-standing records (Ciais et al., 2005; Phillips et al., 2009; Williams et
69 al., 2012; Matusick et al., 2013; Griffin and Anchukaitis, 2014; Asner et al., 2016; Feldpausch et
70 al., 2016; Seneviratne et al., 2021). Such ‘unprecedented climate extremes’ (UCEs; “record-
71 breaking events”, IPCC (2012)) that are larger in extent and longer-lasting than historical norms
72 can have dramatic consequences for terrestrial ecosystem processes, including carbon uptake and
73 storage and other ecosystem services (Reichstein et al., 2013; Settele, 2014; Allen et al., 2015;
74 Brando et al., 2019; Kannenberg et al., 2020). Thus, to better anticipate the implications of
75 climatic changes for the terrestrial carbon sink and other ecosystem services, we need to better
76 understand how ecosystems respond to extreme droughts and other UCEs.

77 To learn how ecosystems respond to rarely experienced or unprecedented conditions,
78 ecologists can experimentally manipulate environmental conditions (Rustad, 2008; Beier et al.,
79 2012; Meir et al., 2015; Aguirre et al., 2021). However, the majority of such experiments apply
80 moderate treatments based on a historical sense, which are mostly weaker in intensity and/or
81 shorter in duration than potential future UCEs (Beier et al., 2012; Kayler et al., 2015; but see Luo
82 et al., 2017), and single experiments have low power to detect effects of stressors on ecosystem
83 responses (Yang et al., 2022). Additionally, most experiments examine low-stature ecosystems,
84 such as grassland, shrubland or tundra, due to lower requirements for infrastructure and financial
85 investment compared to mature forests. However, forests may respond qualitatively differently
86 to UCEs than other ecosystems, in part due to mortality of large trees and strong nonlinear
87 ecosystem responses, with long-lasting consequences for ecosystem-climate feedbacks (Williams
88 et al., 2014; Meir et al., 2015). Ecosystem responses to naturally occurring extreme droughts and
89 heatwaves have been documented (Ciais et al., 2005; Breshears et al., 2009; Feldpausch et al.,
90 2016; Matusick et al., 2016; Ruthrof et al., 2018; Powers et al., 2020); however, these rapidly-
91 mobilized post-hoc studies often are unable to measure all critical variables and may lack
92 consistently collected data for comparison with pre-drought conditions, thus limiting their
93 inferential power and ability to improve quantitative models. The difficulties of performing

94 controlled real-world experiments of UCEs at broad spatial and temporal scales make process-
95 based modeling a valuable tool for studying potential ecosystem responses to extreme events.

96 Process-based models can be used to explore potential ecosystem impacts using projected
97 climate change over broad spatial and temporal scales (Gerten et al., 2008; Luo et al., 2008;
98 Zscheischler et al., 2014; Sippel et al., 2016), as seen in a few modeling studies that have
99 synthesized and improved our process-level understanding of UCE effects (McDowell et al.,
100 2013; Dietze and Matthes, 2014). However, due to the overly simplified representation of
101 ecological processes in most land surface models (LSMs) – the terrestrial components of Earth
102 System Models (ESMs) used for climate projections – it is doubtful whether most of these
103 models adequately capture ecosystem feedbacks and other responses to UCEs (Fisher and
104 Koven, 2020). For example, only a few ESMs in recent coupled model intercomparison projects
105 (CMIP6) (Arora et al., 2020; IPCC 2021) include vegetation demographics (Döscher et al.,
106 2022), and most rely on prescribed, static maps of plant functional types (PFTs) (Ahlström et al.,
107 2012). Other LSMs simulate PFT shifts (i.e., dynamic global vegetation models, DGVMs; Sitch
108 et al., (2008)) based on bioclimatic limits, instead of emerging from the physiology- and
109 competition-based demographic rates that determine resource competition and plant distributions
110 in real ecosystems (Fisher et al., 2018). While a new generation of LSMs with more explicit
111 ecological dynamics and structured demography is emerging (Holm et al., 2020; Koven et al.,
112 2020; Döscher et al., 2022), most current ESMs are limited in ecological detail and realism (e.g.,
113 ecosystem structure, demography, and disturbances). Failing to mechanistically represent
114 mortality, recruitment, and disturbance – each of which influences biomass turnover and carbon
115 (C) allocation (Friend et al., 2014) – limits the ability of these models to realistically forecast
116 ecosystem responses to anomalous environmental conditions like UCEs (Fisher et al., 2018).

117 Evaluating and improving the representation of physiological and ecological processes in
118 ecosystem models is critical for reducing model uncertainties when projecting the effects of
119 UCEs on long-term ecosystem dynamics and functioning. Vegetation demography, plant
120 hydraulics, enhanced representations of plant trait variation, explicit treatments of resource
121 competition (e.g., height-structured competition for light), and representing major disturbances
122 (e.g., extreme drought) have all been identified as critical areas for advancing current models
123 (Scheiter et al., 2013; Fisher et al., 2015; Weng et al., 2015; Choat et al., 2018; Fisher et al.,
124 2018; Blyth et al., 2021) and are necessary advances for realistically representing the ecosystem

125 impacts of UCEs. In this perspectives focused paper we look at the differences in these
126 processes, and how they contribute to uncertainty across multiple temporal phases surrounding
127 an extreme event: predicting an ecosystem's pre-disturbance resistance, which influences the
128 degree of impact and recovery from UCEs. Table 1 describes a summary of model mechanisms
129 that affect pre-drought resistance and post-drought recovery and we suggest are critical areas
130 further research (ca. Frank et al., 2015).

131 In order to inform our discussion, we explore the potential responses of forest ecosystems
132 to UCEs using two state-of-the-art process-based demographic models (vegetation demographic
133 models, VDMs; Fisher et al., (2018)), a unique model exploration-discussion approach to help
134 highlight new paths forward for model advancement. We first present conceptual frameworks
135 and hypotheses on potential ecosystem responses to UCEs based on current knowledge. We then
136 present VDM simulations for a range of hypothetical UCE scenarios to illustrate current state-of-
137 the-art model representations of eco-physiological mechanisms expected to drive responses to
138 UCEs, using droughts as an example. While a variety of UCE-linked biophysical tree
139 disturbance processes (e.g., fire, wind, insect outbreaks) can drive nonlinear ecosystem
140 responses, we focus specifically on extreme droughts, which have important impacts on many
141 ecosystems around the world (e.g. Frank et al., 2015, IPCC 2021). By studying modeled
142 responses to UCEs, we explore the limits to our current understanding of ecosystem responses to
143 extreme droughts and their corresponding thresholds and tipping points. As anthropogenic
144 forcing has increased the frequency, duration, and intensity of droughts throughout the world
145 (Chiang et al., 2021), we explore how eCO₂ and rising temperatures may affect drought-induced
146 C loss and recovery trajectories. This study can help guide how the scientific community can
147 iteratively address these questions through future experiments and modeling studies. We believe
148 the combination of using cutting-edge VDMs alongside an inspection of current gaps in
149 knowledge will help guide modeling and experimental advances in order to address novel forest
150 responses to climate extremes.

151

152 **1.1 Conceptual and Modeling Framework for Hypothesis Testing:**

153 We combine conceptual frameworks (Fig. 1) and ecosystem modeling to test two
154 hypotheses on potential responses of plant carbon stocks to UCEs. The first hypothesis is:

155 ***Hypothesis (H1). Terrestrial ecosystem responses to UCEs will differ qualitatively from***
156 ***ecosystem responses to milder extremes because responses are nonlinear and highly variable.***
157 ***Nonlinearities can arise from multiple mechanisms – including shifts in plant hydraulics, C***
158 ***allocation, phenology, and stand demography – and can vary depending on the pre-drought***
159 ***state of the ecosystem.***

160 We present three conceptual relationships that describe terrestrial ecosystem responses to
161 varying degrees of extreme events (Fig. 1). We hypothesize that change in vegetation C stock is
162 related to drought intensity and/or drought duration, such that biomass loss increases nonlinearly
163 with increased drought intensity (i.e., reduction in precipitation) represented by a threshold-based
164 relationship (Fig. 1a, H1a), increased drought duration (i.e., prolonged drought with the same
165 intensity) by shifting responses typically seen in milder extremes downwards via increasing
166 slopes (Fig. 1a, H1b), or the combination of both intensity and duration (Fig. 1a, H1c). These
167 hypotheses are supported by observations from the Amazon Basin and Borneo (Phillips et al.,
168 2010) where tree mortality rates increased nonlinearly with drought intensity. Similarly, plant
169 hydraulic theories predict nonlinear damage to the plant-water transport systems, and thus
170 mortality risk, as a function of drought stress (Sperry and Love, 2015). In particular, longer
171 droughts are more likely to lead to lower soil water potentials, leading to a nonlinear xylem
172 damage function even if stomata effectively limit water loss (Sperry et al., 2016).

173 ***Hypothesis (H2): The effects of increasing atmospheric CO₂ concentration (eCO₂) will***
174 ***alleviate impacts of extreme drought stress through an increase in vegetation productivity and***
175 ***water-use efficiency, but only up to a threshold of drought severity, while increased***
176 ***temperature (and related water stress) will exacerbate tree mortality.***

177 This second hypothesis is based on growing evidence that effects of eCO₂ and climate
178 warming may interact with effects of drought intensity on ecosystems. The CO₂ fertilization
179 effect enhances vegetation productivity (e.g., net primary production, NPP) (Ainsworth and
180 Long, 2005; Norby et al., 2005; Wang et al., 2012), but this fertilization effect is generally
181 reduced by drought (Hovenden et al., 2014; Reich et al., 2014; Gray et al., 2016). Drought events
182 often coincide with increased temperature, which intensifies the impact of drought on
183 ecosystems (Allen et al., 2015; Liu et al., 2017), resulting in nonlinear responses in mortality
184 rates (Adams et al., 2009; Adams et al., 2017a). The evaluation of C cycling in VDMs with

185 doubling of CO₂ (only “beta effect”) showed a large carbon sink in a tropical forest (Holm et al.,
186 2020), but the inclusion of climate interactions in VDMs needs to be further explored.

187 Here, we relate ecosystem responses to UCEs by calculating a “severity-drought index”
188 (Fig. 1b and see Methods), which integrates C loss from the beginning of the drought until the
189 time when C stocks have recovered to 50% of the pre-drought level. In response to drought,
190 warming, and eCO₂, divergent potential C responses (gains and losses; Fig. 1c) can be expected
191 (Keenan et al., 2013; Zhu et al., 2016; Adams et al., 2017a). For example, a grassland
192 macrocosm experiment found that eCO₂ completely compensated for the negative impact of
193 extreme drought on net carbon uptake due to increased root growth and plant nitrogen uptake,
194 and led to enhanced post-drought recovery (Roy et al., 2016). However, a 16-year grassland
195 FACE and the SoyFACE experiments showed that CO₂ fertilization effects were reduced or
196 eliminated under hotter/drier conditions (Gray et al., 2016; Obermeier et al., 2016). Reich et al.,
197 (2014) also found that CO₂ fertilization effects were reduced in a perennial grassland by water
198 and nitrogen limitation.

199 A corollary to our H2 is that conditions that favor productivity (e.g., longer growing
200 seasons and/or CO₂ fertilization) will enhance vegetation growth leading to “structural
201 overshoot” (SO; Fig. 1d; adapted from and supported by Jump et al., 2017), and can amplify the
202 effects of UCEs. Enhanced vegetation growth coupled with environmental variability can lead to
203 exceptionally high plant-water-demand during extreme drought and water stress, resulting in a
204 “mortality overshoot” (MO; Fig 1d). We conceptualize how oscillations between SO and
205 associated MO could be amplified by increasing climatic variability and UCEs (Fig. 1d).
206 Additionally, more climatic variability from unprecedented eCO₂ levels and warming will
207 contribute to unknowns in how ecosystems are affected in the future (i.e., the widening, and
208 downward shape of the shaded areas compared to historical, Fig. 1d). We expect, however that a
209 rapidly changing climate, combined with effects of UCEs as a result of more frequent extreme
210 drought/heat events and drought stress, can exacerbate and amplify SOs and MOs (Jump et al.,
211 2017), leading to increasing C loss, even though various buffering mechanisms exist (cf. (Lloret
212 et al., 2012; Allen et al., 2015)). Relative to our conceptual (Fig. 1d), we note that most
213 experimental, observational and modeling studies (Ciais et al., 2005; da Costa et al., 2010;
214 Phillips et al., 2010; Meir et al., 2015) take into account only low to moderate drought intensities

215 (such as 50% rain excluded) or single events, or combine drought with moderate effects of
216 temperature change. Where there has been 100% rain exclusion, it was on very small plots of 1.5
217 m² (Meir et al., 2015). As represented by the increasing amplitude of oscillations in Fig. 1d, the
218 interactions between increased temperatures, UCE events, and vegetation feedbacks make
219 ecosystem states become inherently unpredictable, particularly over longer time-scales.

220

221 **2 Vegetation Demography Model (VDM) Approaches**

222 We argue that VDMs are well suited to address climate change impacts due to the
223 inclusion of detailed process representation of dynamic plant growth, recruitment, and mortality,
224 resulting in changes in abundance of different PFTs, as well as vertically stratified tree size- and
225 age-class structured ecosystem demography. Community dynamics and age-/size-structure are
226 emergent properties from competition for light, space, water, and nutrients, which dynamically
227 and explicitly scale up from the tree, to stand, to ecosystem level. Within this characterization,
228 VDMs also differ between each other and are set up in different configuration, allowing for
229 various testing capabilities. For full names of each model listed below and references, see Table
230 S1. For example, VDMs can aggregate and track the community level disturbance into either
231 patch-tiling sampling (e.g., ED2, FATES, LM3-PPA, ORCHIDEE, JSBACH4.0) or statistical
232 approximations (e.g., LPJ-GUESS, SEIB-DGVM, and CABLE-POP). VDMs could also vary in
233 representing light competition within either multiple canopy layers (e.g., ED2, FATES, LM3-
234 PPA, LPJ-GUESS, SEIB-DGVM) or in a single canopy (e.g., JSBACH4.0, ORCHIDEE,
235 CABLE-POP).

236 Powell et al. (2013) compared multiple VDMs and LSMs to interpret ecosystem
237 responses to long-term droughts in the Amazon and are informative when conducting model-data
238 comparisons, but studies of the cascade of ecosystem responses and mortality to UCEs are
239 lacking. In a cutting-edge area of development, new mechanistic implementation of plant
240 competition for water and plant hydraulics in VDMs (i.e., hydrodynamics) are improving our
241 understanding of plant-water relations and stresses within plants, such as with TFSv.1-Hydro
242 (Christoffersen et al., 2016), ED2-hydro (Xu et al., 2016), and FATES-HYDRO (Ma et al., 2021;
243 Fang et al., 2022). Compared to more simplistic representation of plant acquiring soil moisture
244 not connected to plant physiology (e.g., LPJ-GUESS, LM3-PPA, CABLE-POP, SEIB-DGVM).

245 For hydrodynamic representations in ‘big-leaf’ LSMs such as CLM5, JULES, and Noah-MP-
246 PHS see Kennedy et al., (2019), Eller et al., (2020), and Li et al., (2021) respectively.

247 The discussion section provides a deeper investigation of model response to UCEs related
248 to droughts. An exhaustive review of all VDMs, and all plant processes is too large to be done
249 here. Existing review papers of different VDM development, processes, and uncertainties can be
250 found here: Fisher et al., (2018); Bonan (2019); Trugman et al., (2019); Hanbury-Brown et al.
251 (2022); Bugmann and Seidl (2022); and specifically related to plant hydraulics see: Mencuccini
252 et al., (2019); Anderegg and Venturas (2020). We use LPJ-GUESS and ED2 as example VDMs
253 in an initial guide framework to explore hypotheses around vegetation mortality and severity
254 index from UCEs and climate change impacts, and highlight limiting model processes. Since
255 field data needed to evaluate UCE responses are, by definition, unavailable, we do not perform
256 model-data comparisons. Rather, we use the model results and conceptual framework as a road
257 map to explore our hypotheses and illustrate their implications for ecosystem responses under
258 UCEs, not historical drought events.

259

260 **2.1 LPJ-GUESS and ED2 Model Descriptions**

261 We explored our hypotheses at forested ecosystems in Australia and Central America
262 using two VDMs: the Lund-Potsdam-Jena General Ecosystem Simulator (LPJ-GUESS) (Smith et
263 al., 2001; Smith et al., 2014) and the Ecosystem Demography model 2 (ED2) (Medvigy et al.,
264 2009; Medvigy and Moorcroft, 2012). Both LPJ-GUESS and ED2 resolve vegetation into tree
265 cohorts characterized by their PFT, in addition to age-class in LPJ-GUESS; and size, and stem
266 number density in ED2. Both models are driven by external environmental drivers (e.g.,
267 temperature, precipitation, solar radiation, atmospheric CO₂ concentration, nitrogen deposition),
268 and soil properties (soil texture, depth, etc.), and also depend on dynamic ecosystem state, which
269 includes light attenuation, soil moisture, and soil nutrient availability. Establishment and growth
270 of PFTs, and their carbon-, nitrogen- and water-cycles, are simulated across multiple patches per
271 grid cell to account for landscape heterogeneity. Both models characterize PFTs by physiological
272 and bioclimatic parameters, which vary between the models (Smith et al., 2001; Smith et al.,
273 2014; Medvigy et al., 2009; Medvigy and Moorcroft, 2012).

274 The LPJ-GUESS includes three woody PFTs: evergreen, intermediate evergreen, and
275 deciduous PFTs. Mortality in LPJ-GUESS is governed by a ‘growth-efficiency’-based function

276 (kg C m⁻² leaf yr⁻¹), which captures effects of water deficit, shading, heat stress, and tree size on
277 plant productivity relative to its resource-uptake capacity (leaf area), with a threshold below
278 which stress-related mortality risk increases markedly, in addition to background senescence and
279 exogenous disturbances. Stress mortality can be reduced by plants using labile carbon storage,
280 modeled implicitly using a ‘C debt’ approach, which buffers low productivity, enhancing
281 resilience to milder extremes (more details are given in section 4.1.4). Total mortality can thus be
282 impacted by variation in environmental conditions such as water limitation, low light conditions,
283 and nutrient constraints, as well as current stand structure (Smith et al., 2001; Hickler et al.,
284 2004).

285 The ED2 version used here (Xu et al., 2016) includes four woody PFTs: evergreen,
286 intermediate evergreen, deciduous, brevi-deciduous, and deciduous stem-succulent. This ED2
287 version includes coupled photosynthesis, plant hydraulics, and soil hydraulic modules (Xu et al.,
288 2016), which together determine plant water stress. The plant hydraulics module tracks water
289 flow along a soil–plant–atmosphere continuum, connecting leaf water potential, stem sap flow,
290 and transpiration, thus influencing controls on photosynthetic capacity, stomatal closure,
291 phenology, and mortality. Leaf water potential depends on time-varying environmental
292 conditions as well as time-invariant PFT traits. Leaf shedding is triggered when leaf water
293 potential falls below the turgor loss point (a PFT trait) for a sufficient amount of time. Leaf
294 flushing occurs when stem water potential remains high (above half of the turgor loss point) for a
295 sufficient time (see Xu et al., 2016 for details). PFTs differ in their hydraulic traits, wood
296 density, specific leaf area, allometries, rooting depth, and other traits. Stress-based mortality in
297 the ED2 version used here includes two main physiological pathways in our current
298 understanding of drought mortality (McDowell et al., 2013): C starvation and hydraulic failure.
299 Mortality due to C starvation in ED2 results from a reduction of C storage, a proxy for non-
300 structural carbohydrate (NSC) storage, which integrates the balance of photosynthetic gain and
301 maintenance cost under different levels of light and moisture availability. Mortality due to
302 hydraulic failure in ED2 is based on the percentage loss of stem conductivity. ED2 also includes
303 a density-independent senescence mortality rate based on wood density.

304 **2.2 Modeling guide**

305 To exemplify how VDMs can be tools to explore new hypotheses related to UCEs we
306 applied the models at two field sites, that were chosen due to being extensively studied and the
307 models used here have already been run at these sites and previously benchmarked against field
308 data (see Xu et al., 2016; Medlyn et al., 2016; Medvigy et al., 2019 for model-data validation).
309 The purpose of this paper was not to do a large multi-site comparison, but rather just select a few
310 for hypothesis testing. In addition, the two sites span a range of vegetation types and are in
311 warm, seasonally dry climates that are more likely to experience droughts in the future (Allen et
312 al., 2017). The first is a mature *Eucalyptus* (*E. tereticornis*) warm temperate-subtropical
313 transitional forest that is the site of the Eucalyptus Free Air CO₂ enrichment (EucFACE)
314 experiment in Western Sydney, Australia (Medlyn et al., 2016; Ellsworth et al., 2017; Jiang et
315 al., 2020). The second site is a seasonally dry tropical forest in the Parque Nacional Palo Verde
316 in Costa Rica (Powers et al., 2009). Site description details can be found in Supplement Text A.

317 We performed a 100-year “baseline” simulation for each model at each site driven by
318 constant, near ambient, atmospheric CO₂ (400 ppm) and recycled historical site-specific climate
319 data (1992-2011 for EucFACE and 1970-2012 for Palo Verde; Sheffield et al., (2006)), absent of
320 drought treatments. A detailed description of the meteorological data and initial conditions used
321 to drive the models is in the Supplementary Text A. The two models were previously tuned for
322 each site (Xu et al., 2016; Medlyn et al., 2016), and no additional site-level parameter tuning was
323 conducted here due to evaluating responses from hypothetical UCEs. To describe the ecosystem
324 impact of UCEs, we simulated 10 years of pre-drought conditions (continuing from the baseline
325 simulation), followed by drought treatments that differed in intensity and duration, followed by a
326 100-year post-drought recovery period. To explore the effects of drought intensity, we conducted
327 20 different artificial drought intensity simulations, in which precipitation during the whole year
328 is reduced by 5% to 100% of its original amount, in increments of 5%. To explore the effects of
329 drought duration, the 20 different drought intensities are maintained over 1, 2 and 4 years (Table
330 S2). We examined model responses of aboveground biomass, leaf area index (LAI), stem density
331 (number ha⁻¹), plant available soil water (mm), plant C storage (kg C m⁻²), change in stem
332 mortality rate (yr⁻¹), and PFT composition.

333 To explore how temperature, eCO₂ concentration, and UCE droughts influence forest C
334 dynamics individually and in combination, we implemented the following five experimental
335 scenarios, some realistic and others hypothetical, for each model (Table S2): increased

336 temperature only (+2K over ambient), eCO₂ only (600 ppm and 800 ppm), and both increased
 337 temperature and eCO₂ (+2K 600 ppm; +2K 800 ppm). Temperature and eCO₂ manipulations
 338 were applied as step increases over the baseline conditions, and are artificial scenarios, as
 339 opposed to model-generated climate projections.

340

341 **2.3 Linking concepts, hypotheses, and model outcomes**

342 To relate our simulation results to Fig. 1a, we compared the total biomass loss as a result
 343 of each drought treatment by calculating the percentage of biomass reduction at the end of the
 344 drought period relative to the baseline (no drought) simulation. To explicitly consider biomass
 345 recovery rates over time, we calculated “severity-drought index” (Eqs. 1-3), as a result of
 346 drought under current climate, which are determined based on the concepts in Fig. 1b. We
 347 defined “severity-drought index” as the time-integrated carbon in biomass that is lost due to
 348 drought relative to what the vegetation would have stored in the absence of drought. That is, it is
 349 the difference between biomass in the presence of drought (B_d) at time (t) and biomass in the
 350 baseline simulation (no drought; B_{base}), integrated over a defined recovery time period (in kg C
 351 m⁻² yr):

$$\text{Severity-drought index} = \int_{t=t_1}^{t=t_2} (B_{base}(t) - B_d(t)) dt \quad (\text{Eq. 1})$$

352

353 To define the bounds of integration, in Eq. 1, t_1 is defined as the time when the maximum
 354 amount of plant C is lost as a result of the drought:

$$B_{base}(t_1) - B_d(t_1) = \max_t [B_{base}(t) - B_d(t)] \quad (\text{Eq. 2})$$

355

356 Then, t_2 is defined implicitly as the time when 50% of the lost biomass has been recovered
 357 compared to the baseline:

$$B_{base}(t_2) - B_d(t_2) = \frac{1}{2} (B_{base}(t_1) - B_d(t_1)) \quad (\text{Eq. 3})$$

358

359 Since all severity-drought index results are taken as the difference from a non-drought baseline
 360 biomass (B_{base}) and all droughts will result in a loss of C.

361 We also use the severity-drought index as a starting point to examine the role of drought,
 362 temperature and eCO₂ change for moderating or exacerbating the impacts of drought on forest C

363 stocks; i.e., to evaluate the hypotheses illustrated in Fig. 1c. To assess these impacts of changing
364 climates, we calculate a severity-climate index (Eq. 4). Defined as the difference between the
365 severity-drought index due to drought alone (Eqs. 1-3) under present climate, and the severity
366 index due to the combined effects of drought and climate change (i.e., five scenarios of
367 temperature increase and eCO₂), still integrated over time to account for recovery:

368

$$369 \quad \text{Severity-climate index} = \text{Severity-drought index}_{\text{drought}} - \text{Severity-drought index}_{\text{drought+CC}} \quad (\text{Eq. 4})$$

370 Because we expect drought to reduce vegetation C stocks, and thus severity-climate
371 index to be negative, positive values of severity-climate index indicate that changes in climatic
372 drivers ameliorate the C losses from drought (i.e., buffering effects). Negative values of severity-
373 climate index indicate that the climate change scenario leads to either greater C losses or losses
374 that persist for longer amounts of time (i.e., magnitude and/or duration) compared to a simulation
375 with no climate change (i.e., “control” run).

376

377 **3 Results**

378 As a basis for the treatment results presented here, we compared the baseline simulations
379 (prior to drought or climate change treatments) of the two VDMs against observations, and found
380 strong model validation at both sites (Table S3, Fig. S1, Supplemental Text A). These models are
381 well documented and investigated VDMs, with many studies that have looked into parameter
382 uncertainty (see Supplemental Text A for select references that explore model/parameter
383 sensitivity).

384 The models displayed varied nonlinear responses to drought, differing substantially in
385 their behavior and between sites. In general, ED2 shows sensitivity to drought duration
386 (Hypothesis H1b), while LPJ-GUESS shows a stronger sensitivity to drought intensity
387 (Hypothesis H1a). ED2’s sensitivity to the duration of drought was mild at Palo Verde (Fig. 2a),
388 and stronger at EucFACE particularly during the 4-year drought with a strong non-monotonic
389 pattern (see explanation below) (Fig. 2b). When reporting only percentage of biomass loss, ED2
390 predicts close to no UCE response at Palo Verde; with a maximum biomass reduction of only
391 40% during 95% precipitation removal and a 4-year drought event (i.e., UCE). LPJ-GUESS
392 shows threshold tipping patterns highly sensitive to drought intensity. C loss predicted by LPJ-

393 GUESS at Palo Verde reached a threshold at ~65% drought intensity, after which forests exhibit
394 strong biomass losses, up to 100% (Fig. 2a). At the EucFACE site, both models predict a critical
395 threshold of biomass loss at 35%-45% drought intensity, with LPJ-GUESS predicting total
396 biomass loss (up to 100%) after this drought intensity threshold (Fig. 2b). The EucFACE drought
397 threshold is lower than that of the seasonally dry mixed tropical forest in Palo Verde.

398 With respect to C loss over a recovering time period (severity-drought index), the two
399 models predict similar drought responses at Palo Verde (Fig. 2c), but not at EucFACE (Fig. 2d).
400 At Palo Verde, the similarity between models in severity-drought index reflected longer biomass
401 recovery time but less biomass loss in the short-term in ED2 relative to LPJ-GUESS, which
402 predicted greater biomass loss immediately after drought but shorter recovery time. With the
403 exception of the 1-year drought in ED2, both models predict similar severity-drought index
404 across a range of UCEs at Palo Verde, via different pathways. The severity-drought index
405 revealed an exacerbated response to drought duration in ED2 with drought durations greater than
406 one year (Fig. 2c), compared to when only examining loss in biomass at the time of the event
407 (Fig. 2a). The “V”-shaped patterns observed particularly in Fig. 2b, arise from interactions
408 between whole-leaf phenology and stomatal responses to drought in ED2. For drought intensities
409 lower than 40%, stomatal conductance is reduced but leaves are not fully shed. Leaf respiration
410 continues, gradually depleting non-structural C pools, followed by a loss of biomass. However,
411 for higher drought intensities, leaf water potentials quickly become systematically lower than
412 leaf turgor loss points and tree cohorts shed all their leaves. This strategy represents an
413 immediate loss of C via leaf shedding, but spares the cohort from slow, respiration-driven
414 depletion of C stocks.

415

416 **3.1 Predicted model responses to UCE droughts combined with increased temperature** 417 **and/or eCO₂**

418 Relating to our second hypothesis of additional effects of warming and eCO₂, we tested
419 15 treatments in total, repeating the five climate change scenarios for each of the three drought
420 durations. With the addition of climate change impacts, ED2 remained sensitive to the duration
421 of drought, with warming negatively impacting severity-climate index and most consistently
422 during 2- and 4-year drought durations. ED2 predicts that during the 2- and 4-year droughts at
423 EucFACE, losses are exacerbated when accompanied with warming, even with eCO₂, with 600

424 ppm having a more detrimental impact than the more elevated 800 ppm (Fig. 3b-c). The average
425 severity-climate index was $-111.0 \text{ kg C m}^{-2} \text{ yr}$ across all 15 treatments (Table 2). Only during the
426 1-year drought duration did drought plus warming and eCO₂ have a buffering effect on C stocks,
427 seen in four out of our five scenarios but only during relatively modest droughts intensities (Fig.
428 3a; i.e., positive severity-climate index, see also Table 2).

429 The ED2 simulations of the seasonally dry Palo Verde site (Fig. 3d-f), produced less
430 frequent negative impacts on drought and climate change driven C losses compared to
431 EucFACE, with an average severity-climate index of $-53.9 \text{ kg C m}^{-2} \text{ yr}$ across all 15 treatments
432 (Table 2). During the 2-year drought, applying +2K with eCO₂ to 600 ppm showed a slight
433 buffering effect to droughts and the most consistent positive severity-climate index (Fig. 3e;
434 Table 2). Interestingly, an increase in only eCO₂ to 800 ppm (no warming) when applied with the
435 2- and 4-year droughts resulted in the largest loss in carbon (Fig. 3e-f), larger than the expected
436 'most severe' scenario; +2K and 800 ppm.

437 Similar to ED2, the LPJ-GUESS model showed a nearly complete negative response in
438 severity-climate index as a result of UCE drought and scenarios of warming and eCO₂ at the
439 EucFACE site (Fig. 3g-i), but mixed and more muted results at Palo Verde (Fig. 3j-l, Table 2).
440 The average severity-climate index relative to the no climate change control case was -95.4 at
441 EucFACE and $-7.8 \text{ kg C m}^{-2} \text{ yr}$ at Palo Verde, both less negative compared to ED2. One notable
442 pattern was up until a drought intensity threshold of ~40%, the climate scenarios had no effect or
443 response in severity-climate index at EucFACE, and the muted response from warming and
444 eCO₂ Palo Verde, compared to ED2. Surprisingly, the +2K scenario switched the severity-
445 climate index to positive, compared to the control case (Fig. 3g-i; red lines), potentially a
446 physiological process in the model to increased temperatures only that signals an anomalous
447 resiliency response. Similar to the results with no climate change, LPJ-GUESS remained
448 sensitive to the intensity of drought, with ~40% precipitation reduction being a threshold.

449 When comparing the VDM responses to increasing drought severity and its interactions
450 with warming and eCO₂ (related to conceptual Fig. 1d), ED2 showed a more consistent MO
451 response during UCEs and with additional warming and eCO₂ (Fig. 3; negative severity-climate
452 index), especially at EucFACE, suggesting these ecosystems will remain in a depressed carbon
453 condition driving vegetation mortality, and/or longer recoveries. LPJ-GUESS produced more
454 opportunities for SO with climate change. For example, at EucFACE CO₂ fertilization created

455 small SO periods that then led to MO with increasing drought severities, and at Palo Verde all
456 +2K and 600 ppm led to a SO (Fig. 3j-l; Table 2).

457 Both models predicted that C losses due to drought interactions with increased
458 temperature and eCO₂ were less severe at the seasonally dry Palo Verde site compared to the
459 somewhat less seasonal, more humid EucFACE site (Table 2), which could be attributed to
460 higher diversity in PFT physiology at Palo Verde. Palo Verde's community composition that
461 emerged following drought included either three (LPJ-GUESS) or four (ED2) PFTs, while only a
462 single PFT existed at EucFACE. With rising temperatures under climate change, UCEs will be
463 hotter and drier. Nine out of the twelve simulations with both +2K and 600 ppm CO₂, and all but
464 one +2K and 800 ppm CO₂ produced a negative severity-climate index, implying stronger C
465 losses and/or longer recovery times when droughts are exacerbated by increasing temperatures
466 (Table 2).

467

468 **4 Discussion**

469 Vegetation demographic models (VDMs) allowed us to uniquely explore two hypotheses
470 regarding a range of modeled response of terrestrial ecosystems to unprecedented climate
471 extremes (UCEs), and setting the stage for the following perspectives to help guide future
472 research. Key model results indicate strong differences in nonlinearities in C response to extreme
473 drought *intensities* in LPJ-GUESS and alternatively drought *durations* in ED2 (at one of two
474 sites), with differences in thresholds between the two models and ecosystems, and only the ED2
475 model representing impacts from combined intensity and drought (Hypothesis H1c). These
476 nonlinearities may arise from multiple mechanisms that we begin to investigate here, including
477 shifts in plant hydraulics or other functional traits, C allocation, phenology, stand size-structure
478 and/or age demography, and compositional changes, all which vary among ecosystem types. A
479 critical look of driving model mechanisms, which emerged from the hypothetical drought
480 simulations used here, are summarized in Table 3. The models also show exacerbated biomass
481 loss and recovery times in the majority of our scenarios of warming and eCO₂, supporting
482 Hypothesis H2. Below, we discuss the underlying mechanisms that drive simulated ecosystem
483 response to UCEs using the models and sites as conceptual "experimental tools" and
484 observational evidence from the literature. We focus on two temporal stages of the UCE: The
485 pre-drought ecosystem stage characterized as the quasi-stable state of the ecosystem prior to a

486 UCE, which can mediate ecosystem resistance and disturbance impact, and the post-drought
487 recovery stage (Table 1).

488

489 **4.1 The role of ecosystem processes and states prior to UCEs**

490 **4.1.1 The role of phenology and phenological strategies prior to UCEs:**

491 Observations show that diversity of deciduousness contributes to successful alternative
492 strategies for tropical forest response to water stress (Williams et al., 2008). For example, during
493 the severe 1997 El Nino drought, brevi-deciduous trees and deciduous stem-succulents within a
494 tropical dry site in Guanacaste Costa Rica retained leaves during the extreme wet-season
495 drought, behaving differently than during normal dry seasons (Borchert et al., 2002). Both
496 models here predict that neither seasonal deciduousness, nor drought-deciduous phenology at the
497 seasonally dry tropical forest, Palo Verde (which consists of trees with different leaf
498 phenological strategies), act to buffer the forest from a large drop in LAI during UCEs (Fig. S1a-
499 b). Even with this large decrease in LAI, ED2 predicted a very weak biomass loss at the time of
500 UCEs (Fig. 2a), suggesting large-scale leaf loss is not a direct mechanism of plant mortality in
501 ED2. Leaf loss is one component of total carbon turnover flux equations in terrestrial models, in
502 addition to woody loss, fine-roots, and reproductive tissues. Having a better understanding of
503 when extreme levels of phenological turnover contribute to stand-level mortality could be
504 improved. Among other turnover hypothesis explored, Pugh et al. (2020) found that phenological
505 turnover fluxes were just as important as mortality fluxes in driving forest turnover time in the
506 VDMs: LPJ-GUESS, CABLE-POP, ORCHIDEE, but not the LSM JULES. At the EucFACE
507 site prior to the simulated extreme drought, LPJ-GUESS displayed strong inter-annual variability
508 in LAI (Fig. S1a-b). This capability of large swings in LAI (5.8 to 0.8) by LPJ-GUESS could
509 contribute to model uncertainty and the considerable mortality response at EucFACE. Modeled
510 LAI was the largest source of variability in another ecosystem model, CABLE, when evaluating
511 the simulated response to CO₂ fertilization (Li et al., 2018). VDMs could be improved by better
512 capturing different plant phenological responses to UCEs by better representing a range of leaf-
513 level morphological and physiological characteristics relevant to plant-water relations such as
514 leaf age, retention of young leaves even during extreme droughts, (Borchert et al., (2002)), and
515 variation in hydraulic traits as a function of leaf habit (Vargas et al., (2021)) (Table 3). Two such

516 examples are seen in the FATES model where the possibility for “trimming” the lowest leaf
517 layer can occur when leaves are in negative carbon balance due to light limitation thus
518 optimizing maintenance costs and carbon gain, as well as leaf age classifications providing
519 variations in leaf productivity and turnover.

520

521 **4.1.2 The role of plant hydraulics prior to UCEs:**

522 Susceptibility of plants to hydraulic stress is one of the strongest determinants of
523 vulnerability to drought, with loss of hydraulic conductivity being a major predictor of drought
524 mortality in temperate (McDowell et al., 2013; Anderegg et al., 2015; Sperry and Love, 2015;
525 Venturas et al., 2021) and tropical forests (Rowland et al., 2015; Adams et al., 2017b), as well as
526 a tractable mortality mechanism to represent in process-based models (Choat et al., 2018,
527 Kennedy et al., 2019). Both LPJ-GUESS and ED2 exhibited a wide range in amount and pattern
528 of plant-available-water prior to drought (Fig. S1c-d), contributing to large differences in UCE
529 response. LPJ-GUESS, which does not simulate hydrodynamics, predicted lower total plant-
530 available-water at both sites compared to ED2, and subsequently simulated greater mortality and
531 a greater increase in plant-available-water right after the UCEs as a result of less water demand.
532 Due to ED2 using a static mortality threshold from conductivity loss (88%), it likely does not
533 accurately reproduce the wide range of observations of drought-induced mortality. In ED2, large
534 trees, with longer distances to transport water, were at higher risk and suffered higher mortality
535 (Fig. 4), demonstrating how stand demography, size structure, and tapering of xylem conduits
536 can play an important role in ecosystem models (Petit et al., 2008; Fisher et al., 2018). Of the
537 VDMs that are beginning to incorporate a continuum of hydrodynamics (e.g., ED2 (described in
538 Methods 2.1 section) and FATES-HYDRO (Fang et al., 2022, based on Christoffersen et al.,
539 2016), they are able to solve for transient water from soils to roots, through the plant and connect
540 with transpiration demands. Therefore, instead of the plant water stress function being based on
541 soil water potentials, it is replaced with more realistic connections with leaf water potentials.
542 Mortality is then caused by hydraulic failure via embolism controlled by the critical water
543 potential (P_{50}) that leads to 50% loss of hydraulic conductivity. For advancements in tree level
544 hydrodynamic modeling see the FETCH3 model (Silva et al., 2022), for justification for plant
545 hydrodynamics in conjunction with multi-layer vertical canopy profiles see Bonan et al., (2021).
546 There are strong interdependencies and related mechanisms connecting both hydraulic failure

547 (e.g., low soil moisture availability) and C limitation (e.g., stomatal closure) during drought
548 (McDowell et al., 2008; Adams et al., 2017b), and these interactions should be incorporated in
549 ecosystem modeling and further explored (Table 3).

550 **4.1.3. The role of carbon allocation prior to UCEs:**

551 Plants have a variety of strategies to buffer vulnerability to water and nutrient stress
552 caused by extreme droughts, such as allocating more C to deep roots (Joslin et al., 2000; Schenk
553 and Jackson, 2005), investing in mycorrhizal fungi (Rapparini and Peñuelas, 2014), or reducing
554 leaf area without shifting leaf nutrient content (Pilon et al., 1996). Alternatively, presence of
555 deep roots doesn't necessarily lead to deep soil moisture utilization, as seen in a 6-year
556 Amazonian throughfall exclusion experiment where deep root water uptake was still limited,
557 even with high volumetric water content (Markewitz et al., 2010). Elevated CO₂ alone will
558 enhance growth and water-use efficiency (Keenan et al., 2013), reducing susceptibility to
559 drought. However, such increased productivity within a forest stand, and associated structural
560 overshoot during favorable climate windows, can also be reversed by increased competition for
561 light, nutrients, and water during unfavorable UCEs – potentially leading to mortality overshoot
562 (Fig. 1d) and higher C loss. Mortality overshoot, as a result of structural overshoot, could be an
563 explanation for the negative severity-climate index (i.e., C loss) in the majority of eCO₂-only
564 simulations (18 out of 24 scenarios; Table 2).

565 Effects of CO₂ fertilization on plant C allocation strategies are uncertain. As a result,
566 ecosystem models differ in their assumptions on controls of C allocation in response to eCO₂,
567 leading to divergent plant C use efficiencies (Fleischer et al., 2019). Global scale terrestrial
568 models are beginning to include optimal dynamic C allocation schemes, over fixed ratios, that
569 account for concurrent environmental constraints on plants, such as water, and adjust allocation
570 based on resource availability such as in LM3-PPA (Weng et al., 2015), but the representation of
571 C allocation is still debated and progressing (De Kauwe et al., 2014; Montané et al., 2017; Reyes
572 et al., 2017). Options for carbon allocation strategies can be based on the allometric partitioning
573 theory (i.e., allocation follows a power allometry function between plant size and organs which
574 is insensitive to environmental conditions; Niklas, 1993), as an alternative to ratio-based optimal
575 partitioning theory (i.e., allocation to plant organs based on the most limiting resources)
576 (McCarthy and Enquist, 2007) or fixed ratios (Table 3), and the strategies should be further
577 investigated particularly due to VDMs substantial use of allometric relationships. A meta-

578 analysis of 164 studies found that allometric partitioning theory outperformed optimal
579 partitioning theory in explaining drought-induced changes in C allocation (Eziz et al., 2017).
580 Further eco-evolutionarily-based approaches such as optimal response or game-theoretic
581 optimization, as well as entropy-based approaches are useful when wanting to simulate higher
582 levels of complexity (reviewed in Franklin et al. 2012). With more frequent UCEs and the need
583 for plants to reduce water consumption, a shift in the optimal strategy of allocation between
584 leaves and fine roots should change. The goal functions (e.g., fitness proxy) used in optimal
585 response modeling can account for these shifts in costs and benefits of allocation between all
586 organs (Franklin et al. 2009, 2012).

587

588 **4.1.4 The role of plant carbon storage prior to UCEs:**

589 Studies of neotropical and temperate seedlings show that pre-drought storage of non-
590 structural carbohydrates (NSCs) provides the resources needed for growth, respiration
591 osmoregulation, and phloem transport when stomata close during subsequent periods of water
592 stress (Myers and Kitajima, 2007; Dietze and Matthes, 2014; O'Brien et al., 2014). Furthermore,
593 direct correlations have been shown between NSC depletion and embolism accumulation, and
594 the degree of pre-stress reserves and utilization of soluble sugars (Tomasella et al., 2020). The
595 amount of NSC storage required to mitigate plant mortality during C starvation and interactions
596 with hydraulic failure from severe drought is difficult to quantify, due to the many roles of NSCs
597 in plant function and metabolism (Dietze and Matthes, 2014). For example, NSCs were not
598 depleted after 13 years of experimental drought in the Brazilian Amazon (Rowland et al., 2015).
599 As atmospheric CO₂ increases with climate change, NSC concentrations may increase, as seen in
600 manipulation experiments (Coley, 2002), but interactions with heat, water stress, enhanced leaf
601 shedding, and nutrient limitation complicates this relationship, and needs to be further explored.
602 Despite the recognition of the critical role that plant hydraulic functioning and NSCs play in tree
603 resilience to extremes, knowledge gaps and uncertainties preclude fully incorporating these
604 processes into ecosystem models.

605 Compared to ED2, LPJ-GUESS predicted low plant carbon storage (a model proxy for
606 NSCs) prior to and during drought, and at times became negative, thereby creating C costs (Fig.
607 S2a-b), leading to C starvation and potentially explaining the larger biomass loss in LPJ-GUESS
608 at both sites. Alternatively, ED2 maintained higher levels of NSCs providing a buffer to stress,

609 and mitigating the negative effects of drought. Maintenance of NSCs in ED2, even during
610 prolonged drought (at EucFACE) is due to: (1) trees resorbing a fraction of leaf C during leaf
611 shedding, (2) no maintenance costs for NSC storage in the current version, and (3) no allocation
612 of NSCs to structural growth until NSC storage surpasses a threshold (the amount of C needed to
613 build a full canopy of leaves and associated fine roots), allowing for a buffer to accumulate. In
614 LPJ-GUESS, accumulation and depletion of NSC is recorded as a ‘C debt’ being paid back in
615 later years. The contrasting responses of the two models to drought, and the likely role of NSCs
616 in explaining differences in model behavior, highlights the need to better understand NSC
617 dynamics and to accurately represent the relevant processes in models (Richardson et al., 2013;
618 Dietze and Matthes, 2014). More observations of C accumulation patterns and how/where NSCs
619 drive growth, respiration, transport and cellular water relations would enable a more realistic
620 implementation of NSC dynamics in models (Table 3).

621

622 **4.1.5 Role of functional trait diversity prior to UCEs:**

623 Currently LPJ-GUESS simulates the Palo Verde community using three PFTs, while ED2 uses
624 four PFTs that differ in photosynthetic and hydraulic traits. The community composition simulated by
625 ED2 is shown to be more resistant to UCEs compared to LPJ-GUESS (Fig. 5), perhaps due to
626 relatively higher functional diversity (via more PFTs with additional phenological and hydraulic
627 diversity). This additional diversity helps to buffer ecosystem response to drought by allowing more
628 tolerant PFTs to benefit from reductions in less-tolerant PFTs, thus buffering reductions in ecosystem
629 function (Anderegg et al., 2018). Higher diversity ecosystems were found to protect individual species
630 from negative effects of drought (Aguirre et al., 2021) and enhance productivity resilience following
631 wildfire (Spasojevic et al., 2016); thus, functionally diverse communities may be key to enhancing
632 tolerance to rising environmental stress.

633 Recent efforts to consolidate information on plant traits (Reich et al., 2007; Kattge et al., 2011)
634 have contributed to identifying relationships that can impact community-level drought responses
635 (Skelton et al., 2015; Anderegg et al., 2016a; Uriarte et al., 2016; Greenwood et al., 2017), such as
636 life-history characteristics, and strategies of resource acquisition and conservation as predictors of
637 ecosystem resistance (MacGillivray et al., 1995; Ruppert et al., 2015). While adding plant trait
638 complexity in ESMs may be required to accurately simulate key vegetation dynamics, it necessitates
639 more detailed parameterizations of processes that are not explicitly resolved (Luo et al., 2012). Further

640 investigation of how VDMs represent interactions leading to functional diversity shifts is crucial to
641 this issue. Enquist and Enquist, (2011), as an example, show that long-term patterns of drought (20-
642 years) have led to increases in drought-tolerant dry forest species, which could modulate resistance to
643 future droughts. Higher diversity of plant physiological traits and drought-resistance strategies is
644 expected to enhance community resistance to drought, and models should account for shifts in diverse
645 functionality (Table 3).

646

647 **4.2 The role of ecosystem processes and states in post-UCE recovery**

648 **4.2.1 The role of soil water resources post-UCes:**

649 Our simulation results generally demonstrated a fast recovery of plant-available-water
650 and LAI at both sites (Fig. S1). Annual plant-available-water substantially increased right after
651 drought by an average of 163 mm at Palo Verde and 213 mm at EucFACE in the LPJ-GUESS
652 simulations, compared to much lower increases in ED2 (50 mm and 12 mm at Palo Verde and
653 EucFACE). This increase in available water post-drought can be attributed to reduced stand
654 density and water competition (Fig. S2c-d; diamonds vs. circles), alleviating the demand for soil
655 resources (water) and subsequent stress, which has also been shown in observations (McDowell
656 et al., 2006; D'Amato et al., 2013). After large canopy tree mortality events there can be
657 relatively rapid recovery of forest biogeochemical and hydrological fluxes (Biederman et al.,
658 2015; Anderegg et al., 2016b; Biederman et al., 2016). These crucial fluxes strongly influence
659 plant regeneration and regrowth, which can buffer ecosystem vulnerability to future extreme
660 droughts. However, this enhanced productivity has a limit. In a scenario where UCEs continue to
661 intensify, causing greater reductions in soil water and reduced ecosystem recovery potential, the
662 SO growth that typically occurs after UCEs may be dampened (Fig. 1d). In water-limited
663 locations, similar to the dry forest sites used here, initial forest recovery from droughts were
664 faster due to thinning induced competitive-release of the surviving trees, and shallow roots not
665 having to compete with neighboring trees for water, allowing for more effective water user
666 (Tague and Moritz, 2019), stressing the importance of root competition and distribution in
667 models (Goulden and Bales, 2019). Tague and Moritz, (2019) also reported that this increased
668 water use efficiency and SO ultimately lead to water stress and related declines in productivity,
669 similar to the MO concept (Jump et al., 2017; McDowell et al., 2006). Since a core strength of

670 VDMs is predicting stand demography during recovery, improved quantification of density-
671 dependent competition following stand dieback would be beneficial for model benchmarking
672 (Table 3).

673

674 **4.2.2 The role of lagged turnover and secondary stressors post-UCEs:**

675 Time lags in forest compositional response and survival to drought could indicate
676 community resistance or shifts to more competitive species and competitive exclusion. During a
677 15-year recovery period from extreme drought at Palo Verde, LPJ-GUESS predicted an increase
678 in stem density (stems $\text{m}^2 \text{yr}^{-1}$) (Fig. S2c) compared to ED2, which predicted almost no impact in
679 stem recovery. The mortality “spike” in ED2 due to drought was muted and slightly delayed,
680 contributing to ED2’s lower biomass loss and more stable behavior of plant processes over time
681 at Palo Verde. At EucFACE, both models exhibited a pronounced lag effect in stem turnover
682 response, i.e. ~8-12 years after drought (Fig. S2d). After about a decade, strong recoveries and
683 increased stem density occurred, which in ED2 was followed by delayed mortality/thinning of
684 stems. Delayed tree mortality after droughts is common due to optimizing carbon allocation and
685 growth (Trugman et al., 2018), but typically only up to several years post-drought, not a decade
686 or more as seen in the model.

687 The versions of the VDMs used here do not directly consider post-drought secondary
688 stressors such as infestation by insects or pathogens, and the subsequent repair costs due to stress
689 damage, which could substantially slow the recovery of surviving trees. Forest ecologists have
690 long recognized the susceptibility of trees under stress, particularly drought, to insect attacks and
691 pathogens (Anderegg et al., 2015). Tight connections between drought conditions and increased
692 mountain pine beetle activity have been observed (Chapman et al., 2012; Creeden et al., 2014),
693 and can ultimately lead to increased tree mortality (Hubbard et al., 2013). Leaf defoliation is a
694 major concern from insect outbreaks following droughts, and can have large impacts on C
695 cycling, plant productivity, and C sequestration (Amiro et al., 2010; Clark et al., 2010; Medvigy
696 et al., 2012). Implementing these secondary stressors in models could slow the rate of post-UC
697 recovery and lead to increased post-UCEs tree mortality.

698

699 4.2.3 The role of stand demography post-UCEs:

700 Change in stand structure is an important model process to capture, because large trees
701 have important effects on C storage, community resource competition, and hydrology
702 (Wullschleger et al., 2001) (Table 3), and maintaining a positive carbohydrate balance is
703 beneficial in sustaining (or repairing) hydraulic viability (McDowell et al., 2011). There is
704 increasing evidence, both theoretical (McDowell and Allen, 2015) and empirical (Bennett et al.,
705 2015; Rowland et al., 2015; Stovall et al., 2019), that large trees (particularly tall trees with high
706 leaf area) contribute to the dominant fraction of dead biomass after drought events. Under rising
707 temperatures (and decreasing precipitation), VPD will increase, leading to a higher likelihood of
708 large tree death (Eamus et al., 2013; Stovall et al., 2019), driving MO events as hypothesized in
709 Fig. 1d. Consistent with this expectation, ED2 predicted that the largest trees (>100 cm)
710 experienced the largest decreases in basal area to compared to all other size classes (Fig. 4). This
711 drought-induced partial dieback and mortality of large dominant trees has substantial impacts on
712 community-level C dynamics, as long-term sequestered C is liberated during the decay of new
713 dead wood (Palace et al., 2008; Potter et al., 2011). In ED2, the intermediate size class (60 - 80
714 cm) increased in basal area following large-tree death, taking advantage of the newly open
715 canopy space. However, small size classes do not necessarily benefit from canopy dieback. For
716 example, in a dry tropical forest, prolonged drought led to a decrease in understory species and
717 small-sized stems (Enquist and Enquist, 2011).

718 Due to VDMs being able to exhibit dynamic biogeography they are more useful at
719 predicting shifts in community composition beyond LSMs capabilities. Further areas of
720 advancement (described in Franklin et al. (2020)) is including models of natural selection, self-
721 organization, and entropy maximization which can substantially improve community dynamic
722 responses in varying environments such as UCEs. Eco-evolutionary optimality (EEO) theory can
723 also help improve functional trait representation in global process-based models (reviewed in
724 Harrison et al., 2021), through hypotheses in plant trait trade-offs and mechanistic links between
725 processes such as resource demand, acquisition, and plant's competitiveness and survival; traits
726 associated with high degrees of sensitivity in models. The power of prognostic VDMs to predict
727 shifts in demography and community migration with climate change is large, but rarely is being
728 constrained with plant-level EEO theory, and thus will likely need to use stand level competition
729 and coexistence principles of how plants self-organize (Franklin et al. 2020).

730

731 **4.2.4 The role of functional trait diversity & plant hydraulics post-UCEs:**

732 In field experiments, higher disturbance rates have shifted the recovery trajectory and
733 competition of the plant community towards one that is composed of opportunistic, fast-growing
734 pioneer tree species, grasses (Shiels et al., 2010; Carreño-Rocabado et al., 2012), and/or
735 deciduous species, as also seen in model results (Hickler et al., 2004). In the treatments presented
736 here, deciduous PFT types were also the strongest to recover after 15 years in both models,
737 surpassing pre-drought values (Fig. 5). It should be noted that ED2 exhibited a strong recovery in
738 the evergreen PFT as well, inconsistent with the above literature (Fig. 5b). PFTs in ED2 respond
739 to drought conditions via stomatal closure and leaf shedding, buffering stem water potentials
740 from falling below a set mortality threshold (i.e., 88% of loss in conductivity). This conductivity
741 threshold may need to be reconsidered if further examination reveals an unrealistic advantage
742 under drought conditions for evergreen trees, which exhibited a lower impact from droughts
743 (compared to deciduous and brevi-deciduous PFTs) in ED2. Nitrogen cycling feedbacks were
744 not investigated here, but could also be an explanation for a strong evergreen PFT recovery.

745 Recovery of surviving trees could be hindered by the high cost of replacing damaged
746 xylem associated with cavitation (McDowell et al., 2008; Brodribb et al., 2010). Many studies
747 have identified “drought legacy” effects of delayed growth or gross primary productivity
748 following drought (Anderegg et al., 2015; Schwalm et al., 2017) and the magnitude of these
749 legacies across species correlates with the hydraulic risks taken during drought itself (Anderegg
750 et al., 2015). The conditions under which xylem can be refilled remain controversial, but it seems
751 likely that many species, particularly gymnosperms, may need to entirely replace damaged
752 xylem (Sperry et al., 2002), and trees worldwide operate within narrow hydraulic safety margins,
753 suggesting that trees in all biomes are vulnerable to drought (Choat et al., 2012). The amount of
754 damaged xylem from a given drought event and recovery rates also vary across trees of different
755 sizes (Anderegg et al., 2018).

756 Plasticity in nutrient acquisition traits, intraspecific variation in plant hydraulic traits
757 (Anderegg et al., 2015), and changes in allometry (e.g., Huber values) can have large effects on
758 acclimation to extreme droughts. This suggests some capacity for physiological adaptation to
759 extreme drought, as seen by short-term negative effects from drought and heat extremes being

760 compensated for in the longer term (Dreesen et al., 2014). Still, given the shift towards more
761 extreme droughts with climate change, vegetation mortality thresholds are likely to be exceeded,
762 as reported in Amazonian long-term plots where mortality of wet-affiliated genera has increased
763 while simultaneously new recruits of dry-affiliated genera are also increasing (Esquivel-Muelbert
764 et al., 2019). Increasing occurrences of heat events, water stress and high VPD will lead to
765 extended closure of stomata to avoid cavitation, progressively reducing CO₂ enrichment benefits
766 (Allen et al., 2015). Where CO₂ fertilization has been seen to partially offset the risk of
767 increasing temperatures, the risk response was mediated by plant hydraulic traits (Liu et al.,
768 2017) using a soil–plant–atmosphere continuum (SPAC) model, yet interactions with novel
769 extreme droughts were not considered. The VDM simulations suggest that the combination of
770 elevated warming and potential structural overshoot from eCO₂ (or inaccurate representation in
771 NSCs allocation/usage priority) will exacerbate consequences of UCEs by reductions in both C
772 stocks and post-drought biomass recovery speeds (Fig. 3). Therefore, future UCE recovery may
773 not be easily predicted from observations of historical post-disturbance recovery. An associated
774 area for further investigation is to better understand the hypothesized interplay between
775 amplified mortality from hotter UCEs followed by structural overshoot regrowth during wetter
776 periods (Fig. 1d), which could potentially lead to continual large swings in MO and SO and
777 vulnerable net ecosystem C fluxes through time (Table 3).

778

779 **5 Summary of perspectives for model advancement**

780 Model limitations and unknowns exposed by our simulations and literature review
781 highlight current challenges in our ability to understand and forecast UCE effects on ecosystems.
782 These limitations reflect a general lack of empirical experiments focused on UCEs. Insufficient
783 data means that relevant processes may currently be poorly represented in models, and models
784 may then misrepresent C losses during UCEs. The two VDMs used here had different
785 sensitivities to drought duration or intensity, and CO₂ and warming interactions, indicating the
786 wide variety of unknowns and plausible options when trying to represent future UCEs that still
787 needs to be narrowed down (Fig. 1d). These model uncertainties could potentially be addressed
788 by improved datasets on thresholds of conductivity loss at high drought intensities, the role of
789 trait diversity (e.g., different strategies of drought deciduousness and EEO theory) in buffering
790 ecosystem drought responses, and a better grasp of allocation to plant C storage stocks before,

791 during, and after multi-year droughts. Our study takes some initial steps to identify and assess
792 model gaps in terms of mechanisms and magnitudes of responses to UCEs, which can then be
793 used to inform and develop field experiments targeting key knowledge gaps as well as to
794 prioritize ongoing model development (Table 3). Our intention was not to do an exhaustive list
795 of UCE simulation experiments, and additional modeling perturbations and experiments would
796 be useful outcomes of future studies. For example, we begin to investigate duration of droughts
797 but we did not consider frequency of back-to-back UCEs. Using VDMs as hypothesis testing
798 tools offers strong potential to drive progress in improving our understanding of terrestrial
799 ecosystem responses to UCEs and climate feedbacks, while informing the development of the
800 next generation of models.

801 *Code Availability.* The source code for the ED2 model can be downloaded and available publicly
802 at <https://github.com/EDmodel/ED2>. The source code for the LPJ-GUESS model can be
803 downloaded and available publicly at <http://web.nateko.lu.se/lpj-guess/download.html>. All model
804 simulation data will be available in a Dryad repository.
805

806 *Data Availability.* Authors received the required permissions to use the site level meteorological
807 data used in this study. Otherwise, no ecological or biological data were used in this study.
808

809 *Author Contributions.* JH wrote the manuscript with significant contributions from AR, BS, JD,
810 DM, with input and contributions from all authors. XX and MM were the primary leads running
811 the model simulations, with model assistance and strong feedback from DM and BS. All authors
812 made contributions to this article, and agree to submission.
813

814 *Competing Interests.* The contact author has declared that neither they nor their co-authors have
815 any competing interests.
816

817 *Special Issue Statement.* Special Issue titled “Ecosystem experiments as a window to future
818 carbon, water, and nutrient cycling in terrestrial ecosystems”
819

820 *Financial Support:* Funding for the meetings that facilitated this work was provided by NSF-
821 DEB-0955771: An Integrated Network for Terrestrial Ecosystem Research on Feedbacks to the
822 Atmosphere and ClimatE (INTERFACE): Linking experimentalists, ecosystem modelers, and
823 Earth System modelers, hosted by Purdue University; as well as Climate Change Manipulation
824 Experiments in Terrestrial Ecosystems: Networking and Outreach (COST action ClimMani –
825 ES1308), led by the University of Copenhagen. J.A. Holm’s time was supported as part of the
826 Next Generation Ecosystem Experiments-Tropics, funded by the U.S. Department of Energy,
827 Office of Science, Office of Biological and Environmental Research under Contract DE-AC02-
828 05CH11231. AR acknowledges funding from CLIMAX Project funded by Belmont Forum and
829 the German Federal Ministry of Education and Research (BMBF). BS and MM acknowledge
830 support from the Strategic Research Area MERGE. W.R.L.A. acknowledges funding from the
831 University of Utah Global Change and Sustainability Center, NSF Grant 1714972, and the
832 USDA National Institute of Food and Agriculture, Agricultural and Food Research Initiative
833 Competitive Programme, Ecosystem Services and Agro-ecosystem Management, grant no. 2018-
834 67019-27850. JL acknowledges support from the Northern Research Station of the USDA Forest
835 Service (agreement 16-JV-11242306-050) and a sabbatical fellowship from sDiv, the Synthesis
836 Centre of iDiv (DFG FZT 118, 202548816). CDA acknowledges support from the USGS Land
837 Change Science R&D Program.
838

839 *Acknowledgements.* We thank Belinda Medlyn and David Ellsworth of the Hawkesbury Institute
840 for the Environment, Western Sydney University, for providing the meteorological forcing data
841 series for the EucFACE site, a facility supported by the Australian Government through the
842 Education Investment Fund and the Department of Industry and Science, in partnership with
843 Western Sydney University.
844

845 **Table 1.** Hypothesized plant processes and ecosystem state variables affecting pre-drought
846 resistance and post-drought recovery in the context of unprecedented climate extremes (UCEs).
847 The “Included in Model?” column indicates which processes or state variables are represented in
848 each of the two models studied in this paper. The mechanisms listed in the two right columns
849 refer to real-world ecosystems and are not necessarily represented in the ED2 and LPJ-GUESS
850 models. Contents of the table are based on a non-exhaustive literature review, expert knowledge,
851 and modeling results presented here. Symbols refer to the following literature sources: *
852 Borchert et al., 2002; Williams et al., (2008); ** Dietze and Matthes, (2014); O’Brien et al.,
853 2014; *** ENQUIST and ENQUIST, (2011); Greenwood et al., (2017); Powell et al., (2018); ^
854 Rowland et al., (2015); McDowell et al., (2013); Anderegg et al., (2015); ^^ Joslin et al., 2000;
855 Markewitz et al., (2010); ^^^ Powell et al., (2018); ^^^^ Bennett et al., (2015); Rowland et al.,
856 (2015); ~ Hubbard et al., (2013); ~ ~ McDowell et al., (2006); D’Amato et al., (2013); + Zhu et
857 al., (2018); Vargas et al., (2021); % Trugman et al., (2019); %% Franklin et al., (2012); %%
858 Franklin et al., (2020).

Process or State Variable	Included in model?	Mechanisms affecting pre-UCE drought resistance influencing impact	Mechanisms affecting post-UCE drought recovery
Processes			
1) Phenology Schemes	ED2: Yes LPJ-G: Yes	- Leaf area and metabolic activity modulates vulnerability to death - Drought-deciduousness reduces vulnerability to drought *, with higher water potential at turgor loss point and less leaf vulnerability to embolism +	- Leaf lifespan tends to increase from pioneer to late-successional species in some ecosystems (e.g., tropical forests) and is a balance between C gain and its cost
2) Plant Hydraulics	ED2: Yes LPJ-G: No	- Cavitation resistance traits ^ - Turgor loss, hydraulic failure (stem embolism) lead to increased plant mortality and enhanced vulnerability to secondary stressors.	- Replacement cost of damaged xylem slows recovery of surviving trees
3) Dynamic Carbon Allocation	ED2: Yes LPJ-G: Yes	- Increased root allocation could offset soil water deficit under gradual onset of drought ^^ - Leaf C allocation strategies should be connected to hydraulic processes %	- Allocation among fine roots, xylem, & leaves affects recovery time & GPP/LAI trajectory - Eco-evolutionary optimality theory %%

4) Non-Structural Carbohydrate (NSC) Storage	ED2: Yes LPJ-G: Yes	- NSCs buffer C starvation mortality due to reduced primary productivity. - Maintenance of hydraulic function & avoiding hydraulic failure **	- Low NSC could increase vulnerability to secondary stressors during recovery
State Variables			
1) Plant-Soil Water Availability	ED2: Yes LPJ-G: Partly	- Low soil water potential increases risk of tree C starvation, turgor loss and hydraulic failure	- After stand dieback reduced demand for soil resources &/or reduced shading - Increased soil water enhances regeneration/ regrowth, buffers vulnerability to long-term drought ~ ~
2) Plant Functional Diversity	ED2: Yes LPJ-G: Yes	- Presence of drought-tolerant species modulates resistance at community level. - Shallow-rooting species more vulnerable ^^ ^***	- Changed resource spectra shift competitive balance in favor of grasses and pioneer trees
3) Stand Demography	ED2: Yes LPJ-G: Yes	- Larger tree size enhances vulnerability to drought and secondary stressors due to higher maintenance costs ^^ ^^	- Mortality of canopy individuals favors understory species and smaller size-classes - Self-organizing principles %%%
4) Compounding Stressors	ED2: No LPJ-G: No	- Reduced resistance to insects and pathogens due to physiological/mechanical/ hydraulic damage & depletion of NSC	- Infestation by insects and pathogens, repair of damage due to secondary stressors, slows recovery of surviving trees ~

860 **Table 2** Impact of eCO₂ and/or temperature on the severity-climate index (kg C m⁻² yr) relative
861 to drought treatments with no additional warming or eCO₂, for both models, and both sites seen
862 in Fig. 3. Quantified as average and minimum severity-climate index across all 20 drought
863 intensities for step-change scenarios of warming and eCO₂. The percentage of each scenario that
864 was negative in severity-climate index (i.e., decreases in C loss). Green values represent positive
865 severity-climate index.

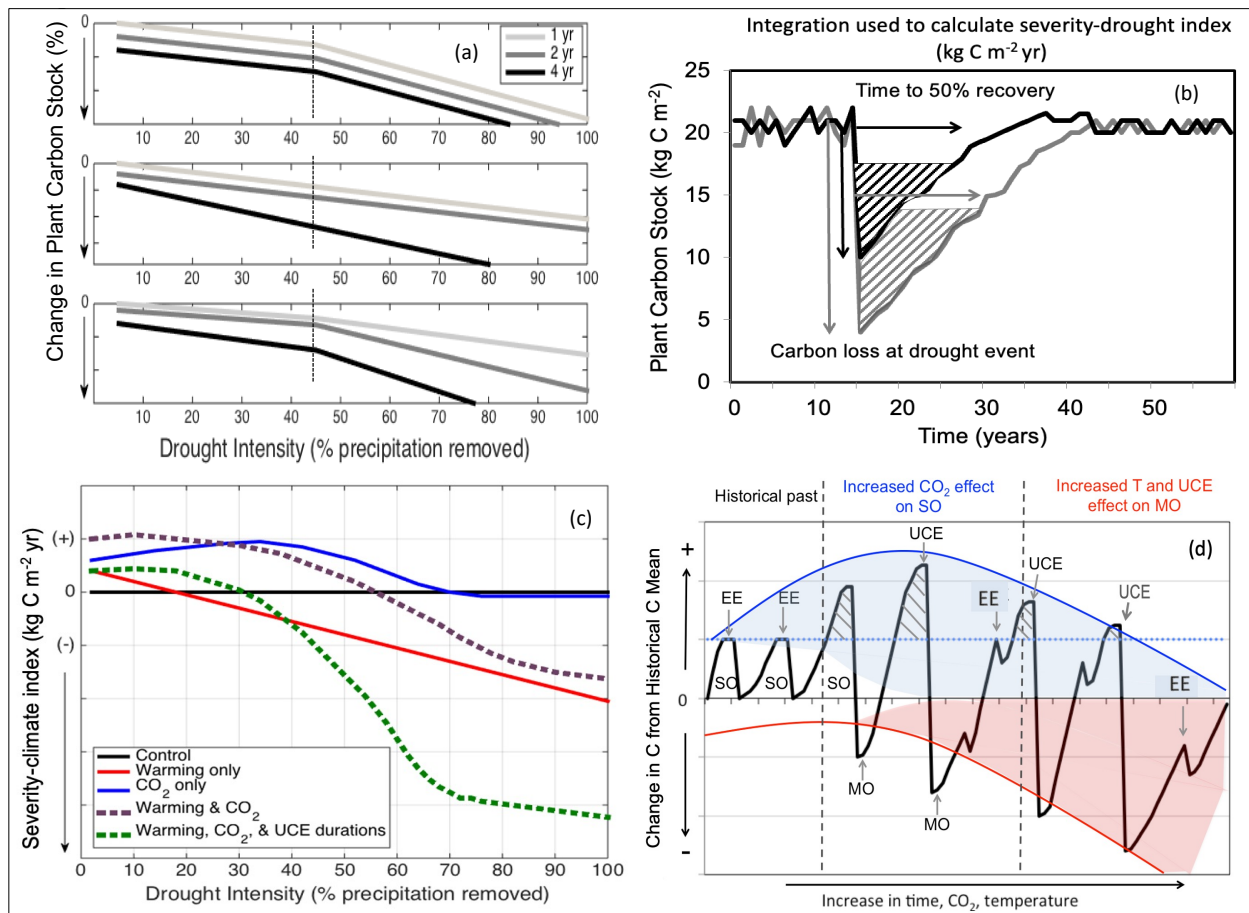
<i>EucFACE</i>		<i>ED2</i>			<i>LPJ-GUESS</i>		
		Average severity-climate index	Largest severity-climate index	% climate scenario was negative	Average severity-climate index	Largest severity-climate index	% climate scenario was negative
1 year	600 ppm	2.2	0.0	33.3	-74.6	-396.6	36.8
	800 ppm	-10.6	-73.0	50.0	-124.1	-416.0	57.9
	2K	2.3	-0.5	16.7	21.3	-20.8	15.8
	2K, 600 ppm	0.5	-8.2	61.1	-67.5	-201.5	78.9
	2K, 800 ppm	1.8	-0.4	22.2	-145.9	-400.1	47.4
2 year	600 ppm	-105.6	-456.7	77.8	-85.2	-260.6	63.2
	800 ppm	-199.0	-522.9	83.3	-106.3	-350.1	42.1
	2K	-10.3	-34.7	77.8	14.2	-35.2	31.6
	2K, 600 ppm	-204.9	-666.1	77.8	-47.6	-128.8	84.2
	2K, 800 ppm	-12.4	-61.6	50.0	-167.0	-421.9	68.4
4 year	600 ppm	-125.5	-306.2	83.3	-122.6	-277.4	94.7
	800 ppm	-277.1	-423.3	100.0	-212.2	-523.7	89.5
	2K	-61.8	-188.6	72.2	12.9	-13.8	31.6
	2K, 600 ppm	-385.9	-674.2	94.4	-79.1	-197.3	94.7
	2K, 800 ppm	-277.9	-737.7	72.2	-247.0	-503.8	100.0
Average		-111.0	-277.0	64.8	-95.4	-276.5	62.5
<i>Palo Verde</i>		<i>ED2</i>			<i>LPJ-GUESS</i>		
1 year	600 ppm	-1.6	-6.2	77.8	-11.0	-32.4	78.9
	800 ppm	6.7	-0.2	11.1	-39.2	-154.0	100.0
	2K	-1.0	-15.3	38.9	-33.4	-75.1	100.0
	2K, 600 ppm	2.5	-1.1	22.2	6.5	-4.6	52.6
	2K, 800 ppm	-6.6	-16.6	77.8	-121.1	-237.7	100.0
2 year	600 ppm	15.1	-16.7	38.9	27.3	-6.0	10.5
	800 ppm	-229.2	-756.6	66.7	20.6	-17.2	26.3
	2K	-8.2	-71.8	50.0	32.0	-12.7	15.8
	2K, 600 ppm	24.8	-5.7	11.1	36.2	-1.2	5.3
	2K, 800 ppm	-152.9	-348.1	77.8	8.0	-54.5	36.8
4 year	600 ppm	-11.1	-37.3	94.4	3.4	-25.1	26.3
	800 ppm	-260.2	-694.8	94.4	-25.2	-132.6	57.9
	2K	-39.0	-133.8	66.7	-7.7	-45.9	68.4
	2K, 600 ppm	1.0	-16.4	38.9	6.1	-4.1	31.6
	2K, 800 ppm	-148.5	-429.3	83.3	-20.0	-75.5	78.9
Average		-53.9	-170.0	56.7	-7.8	-58.6	52.6

866

867 **Table 3** Summary of suggested critical look of driving mechanisms (e.g., ecosystem or plant
 868 processes and state variables) which emerged from the hypothetical drought simulations used
 869 here to explore for future research in manipulation experiments, data collection, and model
 870 development and testing, as related to furthering our understanding of UCE resistance and
 871 recovery.

UCE Drought Resistance & Recovery Summary	
Processes	Suggestions of driving mechanisms to further explore in data and models
1) Phenology Schemes	Represent morphological and physiological traits relevant to plant-water relations; drought- deciduousness can reduce vulnerability to drought; phenology of evergreens needs more investigation.
2) Plant Hydraulics	Interactions between hydraulic failure (e.g. low soil moisture availability) and C limitation (e.g. stomatal closure) during drought should be included in models. Account for turgor loss, hydraulic failure traits, costs to recover damaged xylem.
3) Dynamic Carbon Allocation	C allocation based on eco-evolutionary optimality (EEO) and allometric partitioning theory in addition to, or replacing ratio-based optimal partitioning theory, and fixed allocation ratios. Explore root allocation that could offset soil water deficits.
4) Non-structural Carbohydrate (NSC) Storage	Deciding best practices for NSC representation in models. Better understanding of NSC storage required to mitigate plant mortality during C starvation and interactions with avoiding hydraulic failure during severe droughts.
States Variables	
1) Plant-Soil Water Availability	Better quantification of the amount and accessibility of plant-available water for surviving trees, and tradeoff between increased structural productivity but vulnerability to subsequent droughts. Future relevance, or benefit, of lower water demand due to thinning with UCEs.
2) Plant Functional Diversity	Understand how higher diversity of plant physiological traits and drought-resistance strategies will enhance community resistance to drought; models still need to account for shifts in diverse functionality, including deciduousness shifts and interplay of regrowth structural overshoot followed by amplified mortality from hotter UCEs.
3) Stand Demography	Large trees more vulnerable to drought; need data on changes in C stock with UCEs in high-density smaller tree stands vs. stands with larger trees. Using ‘self-organization’ principles for modeling stand level competition and coexistence under UCEs.

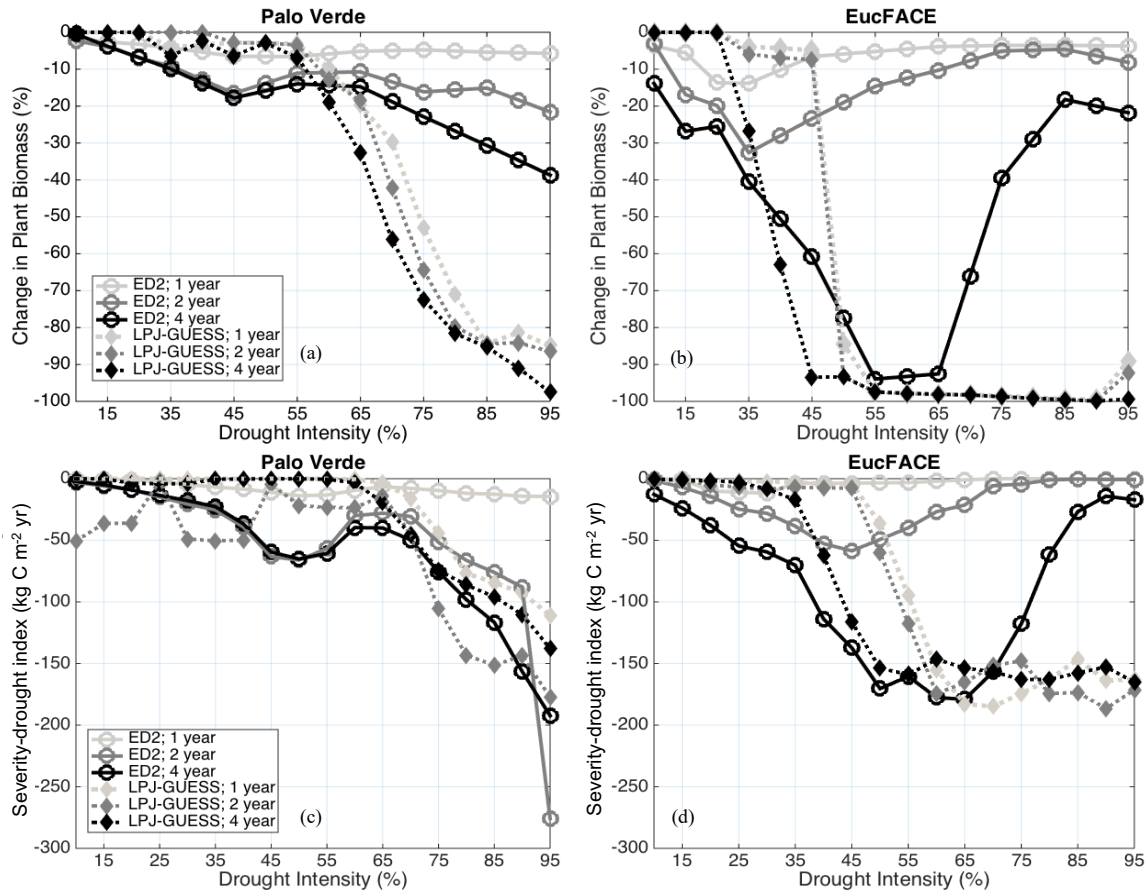
872



874

875 **Figure 1** Conceptual diagrams showing impacts of extreme droughts (unprecedented climate
 876 extremes, UCEs; i.e., record-breaking droughts) on plant C stocks. (a) **Conceptual diagram of**
 877 **UCE C loss:** potential loss in C stock as a function of increasing drought intensity (0-100%
 878 precipitation removal) and drought duration (1, 2 or 4 years of drought). In this example, an
 879 arbitrary threshold of 45% precipitation reduction and 4-year drought duration is assumed to
 880 correspond to a UCE. Hypotheses include nonlinear and threshold responses to drought intensity
 881 (H1a), drought duration via different slope responses (H1b), and combined effects of both
 882 drought intensity and durations (H1c). (b) **Conceptualized diagram of integrated C change:**
 883 responses of forest C stocks to a large (grey) and small (black) UCE. “Severity-drought index”
 884 (kg C m⁻² yr) denotes the integral of the C loss over time and is calculated from the two arrows:
 885 the total loss in C (kg C m⁻²) due to drought, and the time (yr) to recover 50% of the pre-drought
 886 C stock. (c) **Conceptualized UCE-climate C change diagram:** hypothetical response in
 887 terrestrial “severity-climate index” (kg C m⁻² yr) due to eCO₂ (blue line), rising temperature (red
 888 line), interaction between eCO₂ and temperature (dashed purple), and combined interactions

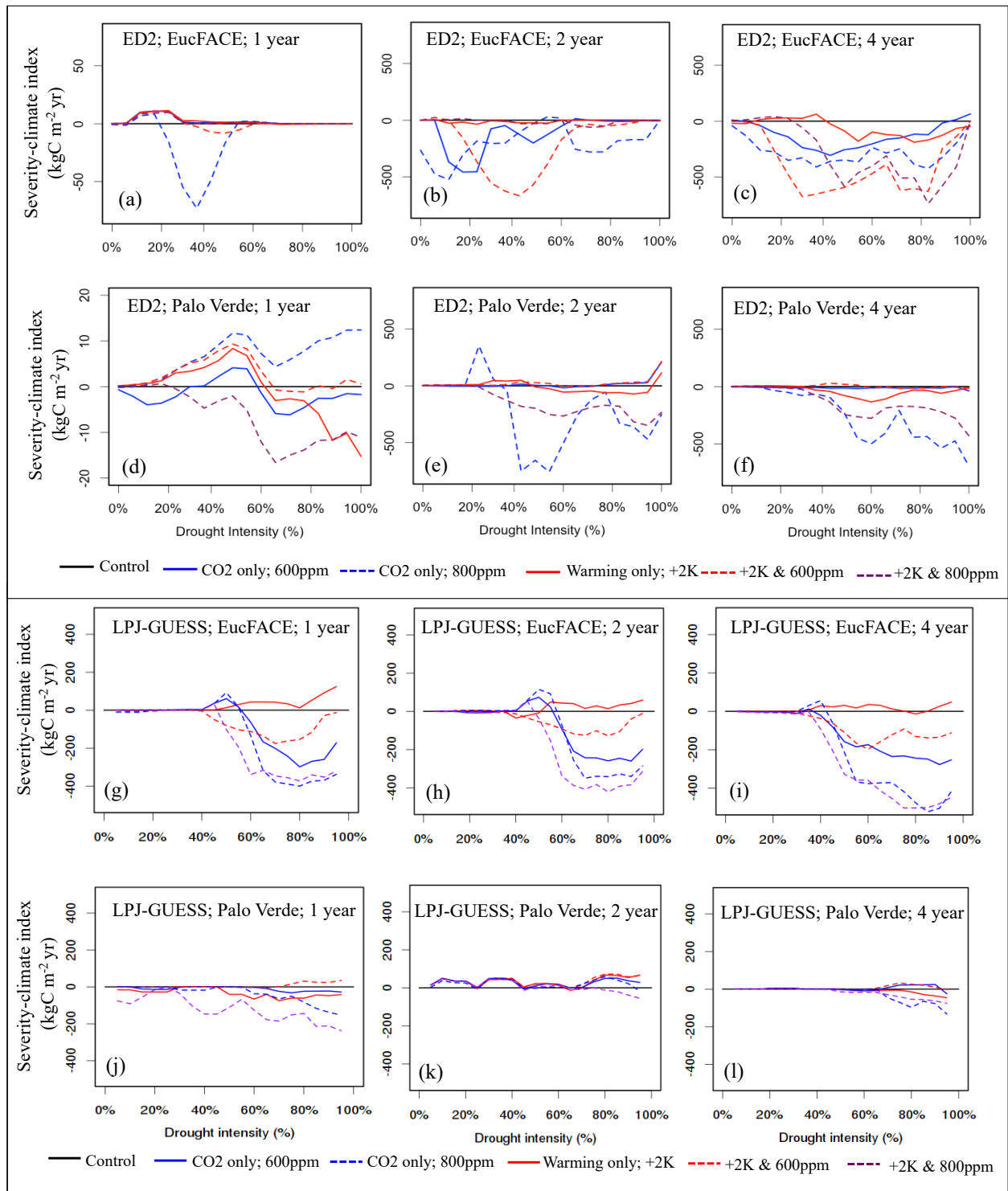
889 among eCO₂, temperature, and UCEs of prolonged durations (green line), all relative to a
890 reference drought of normal duration with no warming (black line). Severity-climate index
891 denotes the difference in severity-drought index (see panel b) between a scenario of changing
892 climatic drivers and the reference drought with no climate change (control). (d) **Conceptual**
893 **UCE amplification diagram:** hypothetical amplified change in forest C stocks to eCO₂ and
894 temperature relative to the pre-warming historical past (based on Jump et al. (2017)). Change in
895 C stock greater than zero indicates a ‘structural overshoot’ (SO) due to favorable environmental
896 conditions and/or recovery from an extreme drought-heat event (EE). Hashed black areas
897 indicate a structural overshoot due to eCO₂, which occurs over the historical CO₂ levels (dashed
898 blue line). Initially, an eCO₂ effect leads to a larger increase in structural overshoot (due to CO₂
899 fertilization), driving more extreme vegetation mortality (‘mortality overshoot’ - MO) relative to
900 historical dieback events and thus a greater decrease in C stock. Increased warming through time
901 increasingly counteracts any CO₂ fertilization effect. While the amplitude of post-UCE C stock
902 recoveries remains large, net C stock values eventually decline (downward curvature, and
903 widening of the red shaded area) due to more pronounced loss in C stocks (and greater
904 ecosystem state change) from hotter UCEs and longer recovery periods. We conceptualize how
905 oscillations between SOs and MOs could be amplified and the widening of the shaded areas
906 represents increased variability in how unprecedented eCO₂ levels and temperatures will affect
907 ecosystems in the future compared to historical.
908 SO = structural overshoot, MO = mortality overshoot, EE = historically extreme drought-heat
909 event, UCE = unprecedented climate extreme.
910



911

912 **Figure 2** Modeled change in biomass (%) at the end of drought periods of different lengths (1, 2,
 913 and 4-year droughts) and intensities (up to 95% precipitation removed) at (a) Palo Verde, and (b)
 914 EucFACE, for the ED2 and LPJ-GUESS models. Modeled severity-drought index (C reduction
 915 due to extreme drought integrated over time until biomass recovers to 50% of the non-drought
 916 baseline biomass) at (c) Palo Verde and (d) EucFACE.

917



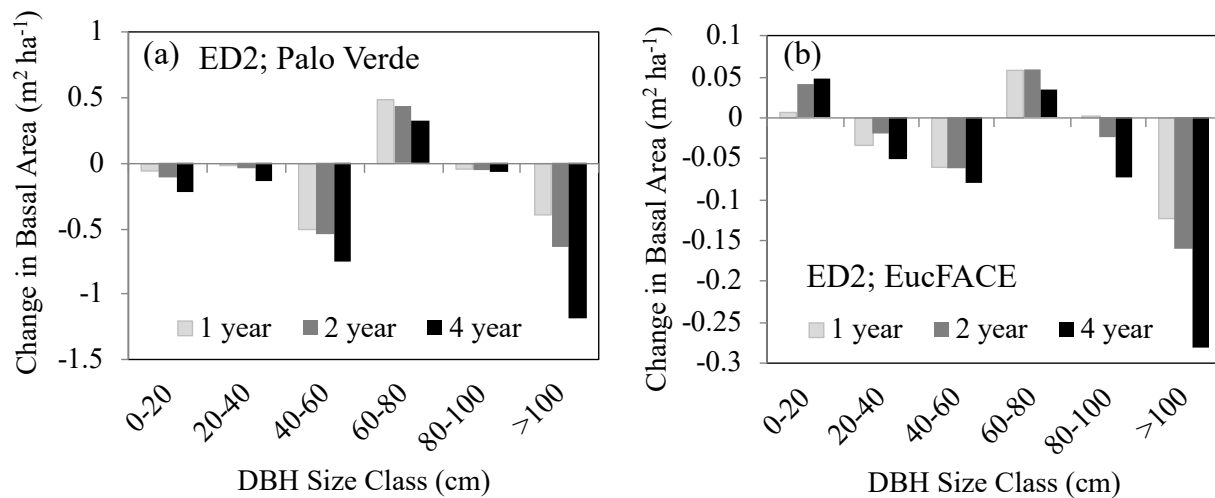
918

919 **Figure 3** Vegetation C response to interactions between drought intensity (0% to 100%
 920 precipitation reduction), drought durations (1, 2, 4-year droughts), and idealized scenarios of
 921 warming and eCO₂ compared to the control simulation, simulated by two VDMs; ED2 (a-f) and
 922 LPJ-GUESS (g-l) at two sites (EucFACE and Palo Verde). The scenarios include a control

923 (current temperature; 400 ppm atmospheric CO₂), two eCO₂ scenarios (600 ppm or 800 ppm),
 924 elevated temperature (2 K above current), and a combination of eCO₂ (600 ppm or 800 ppm) and
 925 higher temperature. Vegetation response is quantified as “severity-climate index” (in kg C m⁻²
 926 yr; Eq. 4), which is defined as the difference between severity-drought index (i.e., carbon loss
 927 due to only drought) and a given scenario of drought plus change in climatic drivers, relative to
 928 the control (i.e., no climate change). Negative values for severity-climate index indicate that
 929 warming and/or eCO₂ leads to stronger C losses and/or longer recovery, while positive values for
 930 severity-climate index indicates a buffering effect.

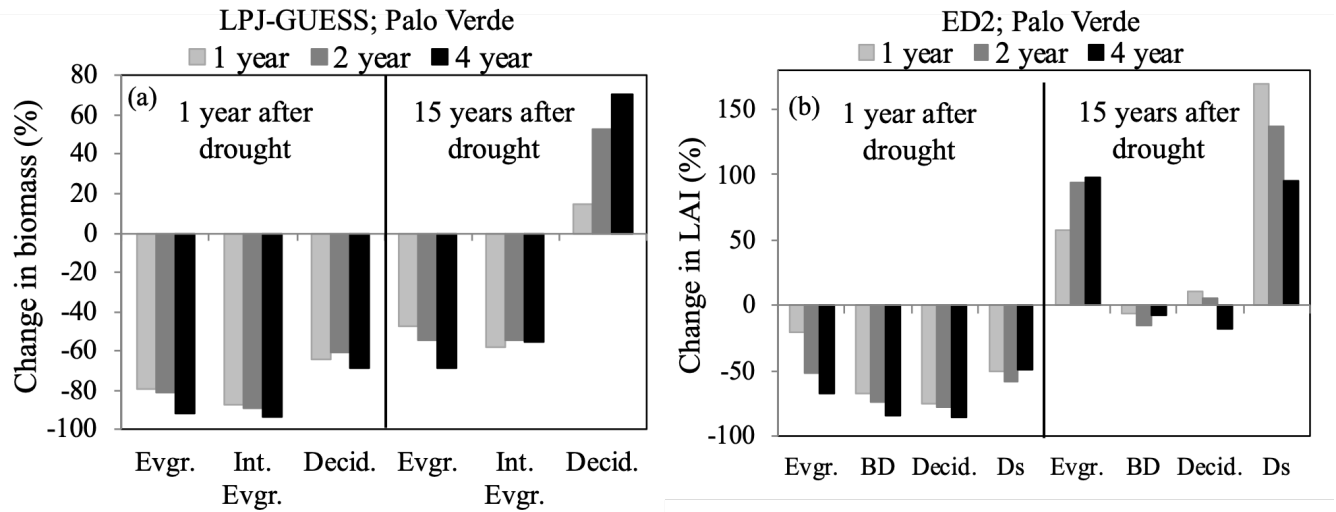
931

932



933

934 **Figure 4** Change in basal area (m² ha⁻¹) immediately following either 1, 2, or 4 year droughts for
 935 six increasing size class bins (DBH, cm) as predicted by the ED2 model for (a) the Palo Verde
 936 site, with 90% precipitation removed, and (b) the EucFACE site with 50% precipitation
 937 removed.



939
940

941 **Figure 5** Percent change in community composition, represented by plant functional type (PFT),
 942 the year following three drought durations of UCEs (1, 2, and 4-year droughts and 90%
 943 precipitation removed) as well as 15 years after droughts, for the tropical Palo Verde site by (a)
 944 LPJ-GUESS reported in biomass change, and (b) ED2 reported in LAI change. Even though Ds
 945 had the strongest recovery, it should be noted it was the least abundant PFT at this site. Evgr. =
 946 evergreen, Int. Ever. = intermediate evergreen, Decid. = deciduous, BD = brevi-deciduous, Ds =
 947 deciduous stem-succulent. EucFACE data not shown because only one PFT present (evergreen
 948 tree).

949 References:

950

951 Adams, H.D., Guardiola-Claramonte, M., Barron-Gafford, G.A., Villegas, J.C., Breshears, D.D.,
952 Zou, C.B. et al.: Temperature sensitivity of drought-induced tree mortality portends
953 increased regional die-off under global-change-type drought, *PNAS*, 106, 7063-7066, 2009.

954 Adams, H.D., Barron-Gafford, G.A., Minor, R.L., Gardea, A.A., Bentley, L.P., Law, D.J. et al.:
955 Temperature response surfaces for mortality risk of tree species with future drought,
956 *Environ. Res. Lett.*, 12, 115014, 2017a.

957 Adams, H.D., Zeppel, M.J.B., Anderegg, W.R.L., Hartmann, H., Landhäusser, S.M., Tissue, D.T.
958 et al.: A multi-species synthesis of physiological mechanisms in drought-induced tree
959 mortality, *Nature Ecol. & Evol.*, 1, 1285-1291, 2017b.

960 Aguirre, BA, Hsieh, B, Watson, SJ, Wright, AJ.: The experimental manipulation of atmospheric
961 drought: Teasing out the role of microclimate in biodiversity experiments, *J. Ecol.*, 109,
962 1986– 1999, <https://doi.org/10.1111/1365-2745.13595>, 2021.

963 Ahlström, A., Schurgers, G., Arneeth, A., and Smith, B.: Robustness and uncertainty in terrestrial
964 ecosystem carbon response to CMIP5 climate change projections, *Environ. Res. Lett.*, 7,
965 044008, 2012.

966 Ainsworth, E.A., and Long, S.P.: What have we learned from 15 years of free-air CO₂
967 enrichment (FACE)? A meta-analytic review of the responses of photosynthesis, canopy
968 properties and plant production to rising CO₂, *New Phytol.*, 165, 351-372, 2005.

969 Allen, C.D., Breshears, D.D., and McDowell, N.G.: On underestimation of global vulnerability to
970 tree mortality and forest die-off from hotter drought in the Anthropocene, *Ecosphere*, 6,
971 art129, 2015.

972 Allen, K., Dupuy, J.M., Gei, M.G., Hulshof, C.M., Medvigy, D., Pizano, C. et al.: Will seasonally
973 dry tropical forests be sensitive or resistant to future changes in 558 rainfall regimes?
974 *Environ. Res. Lett.*, 12, 023001, 2017.

975 Amiro, B.D., Barr, A.G., Barr, J.G., Black, T.A., Bracho, R., Brown, M. et al.: Ecosystem carbon
976 dioxide fluxes after disturbance in forests of North America, *J. Geophys. Res.*
977 *Biogeosciences*, 115, 2010.

978 Anderegg, W.R.L., Hicke, J.A., Fisher, R.A., Allen, C.D., Aukema, J., Bentz, B. et al.: Tree
979 mortality from drought, insects, and their interactions in a changing climate, *New Phytol.*,
980 208, 674-683, 2015.

981 Anderegg, W.R.L., Klein, T., Bartlett, M., Sack, L., Pellegrini, A.F.A., Choat, B. et al.: Meta-
982 analysis reveals that hydraulic traits explain cross-species patterns of drought-induced tree
983 mortality across the globe, *PNAS*, 113, 5024-5029, 2016a.

984 Anderegg, W.R.L., Martinez-Vilalta, J., Cailleret, M., Camarero, J.J., Ewers, B.E., Galbraith, D.
985 et al.: When a Tree Dies in the Forest: Scaling Climate-Driven Tree Mortality to Ecosystem
986 Water and Carbon Fluxes, *Ecosystems*, 19, 1133-1147, 2016b.

987 Anderegg, W.R.L., Konings, A.G., Trugman, A.T., Yu, K., Bowling, D.R., Gabbitas, R. et al.:
988 Hydraulic diversity of forests regulates ecosystem resilience during drought, *Nature*, 561,
989 538-541, 2018.

990 Anderegg, W.R.L. and Venturas, M.D.: Plant hydraulics play a critical role in Earth system
991 fluxes, *New Phytol*, 226, 1535-1538, <https://doi.org/10.1111/nph.16548>, 2020.

992 Asner, G.P., Brodrick, P.G., Anderson, C.B., Vaughn, N., Knapp, D.E., and Martin, R.E.:
993 Progressive forest canopy water loss during the 2012–2015 California drought. *PNAS*, 113,
994 E249-E255, 2016.

- 995 Arora, V.K., Katavouta, A., Williams, R.G., Jones, C.D., Brovkin, V., Friedlingstein, P., et al.:
996 Carbon-concentration and carbon-climate feedbacks in CMIP6 models and their
997 comparison to CMIP5 models, *Biogeosciences*, 17, 4173–4222, 2020.
- 998 Bai, Y., Wu, J., Xing, Q., Pan, Q., Huang, J., Yang, D. et al.: PRIMARY PRODUCTION AND
999 RAIN USE EFFICIENCY ACROSS A PRECIPITATION GRADIENT ON THE
1000 MONGOLIA PLATEAU, *Ecology*, 89, 2140-2153, 2008.
- 1001 Beier, C., Beierkuhnlein, C., Wohlgemuth, T., Penuelas, J., Emmett, B., Körner, C. et al.:
1002 Precipitation manipulation experiments – challenges and recommendations for the future,
1003 *Ecol. Lett.*, 15, 899-911, 2012.
- 1004 Bennett, A.C., McDowell, N.G., Allen, C.D., and Anderson-Teixeira, K.J.: Larger trees suffer
1005 most during drought in forests worldwide, *Nature Plants*, 1, 15139, 2015.
- 1006 Biederman, J.A., Meixner, T., Harpold, A.A., Reed, D.E., Gutmann, E.D., Gaun, J.A. et al.:
1007 Riparian zones attenuate nitrogen loss following bark beetle-induced lodgepole pine
1008 mortality, *J. Geophys. Res. Biogeosciences*, 121, 933-948, 2016.
- 1009 Biederman, J.A., Somor, A.J., Harpold, A.A., Gutmann, E.D., Breshears, D.D., Troch, P.A. et al.:
1010 Recent tree die-off has little effect on streamflow in contrast to expected increases from
1011 historical studies, *Water Resources Res.*, 51, 9775-9789, 2015.
- 1012 Blyth, E.M., Arora, V.K., Clark, D.B. et al.: Advances in Land Surface Modelling, *Curr. Clim.*
1013 *Change Rep.*, 7, 45–71, <https://doi.org/10.1007/s40641-021-00171-5>, 2021.
- 1014 Borchert, R., Rivera, G., and Hagnauer, W.: Modification of Vegetative Phenology in a Tropical
1015 Semi-deciduous Forest by Abnormal Drought and Rain, *Biotropica*, 34, 27-39, 2002.
- 1016 Bonan, G.: Vegetation Demography, in: *Climate Change and Terrestrial Ecosystem Modeling*,
1017 Cambridge: Cambridge University Press, 344-364, doi:10.1017/9781107339217.020, 2019.
- 1018 Bonan, G. B., Patton, E. G., Finnigan, J. J., Baldocchi, D. D., and Harman, I. N.: Moving beyond
1019 the incorrect but useful paradigm: reevaluating big-leaf and multilayer plant canopies to
1020 model biosphere-atmosphere fluxes – a review, *Agr. Forest Meteorol.*, 306,
1021 108435, <https://doi.org/10.1016/j.agrformet.2021.108435>, 2021.
- 1022 Brando, P.M., Paolucci, L., Ummenhofer, C.C., Ordway, E.M., Hartmann, H., Cattau, M.E.,
1023 Rattis, L., Medjibe, V., Coe, M.T., Balch, J.: Droughts, Wildfires, and Forest Carbon
1024 Cycling: A Pantropical Synthesis, *Annual Review of Earth and Planetary Sciences*, 47, 555-
1025 581, 2019.
- 1026 Breshears, D.D., Myers, O.B., Meyer, C.W., Barnes, F.J., Zou, C.B., Allen, C.D. et al.: Tree die-
1027 off in response to global change-type drought: mortality insights from a decade of plant
1028 water potential measurements, *Front. Ecol. Environ.*, 7, 185-189, 2009.
- 1029 Brodribb, T.J., Bowman, D.J.M.S., Nichols, S., Delzon, S. and Burlett, R.: Xylem function and
1030 growth rate interact to determine recovery rates after exposure to extreme water deficit, *New*
1031 *Phytol.*, 188, 533-542, 2010.
- 1032 Bugmann, H., and Seidl, R.: The evolution, complexity and diversity of models of long-term
1033 forest dynamics. *J. of Ecol.*, 110, 2288– 2307, <https://doi.org/10.1111/1365-2745.13989>,
1034 2022.
- 1035 Carreño-Rocabado, G., Peña-Claros, M., Bongers, F., Alarcón, A., Licona, J.-C., and Poorter, L.:
1036 Effects of disturbance intensity on species and functional diversity in a tropical forest, *J.*
1037 *Ecology*, 100, 1453-1463, 2012.
- 1038 Chapman, T.B., Veblen, T.T., and Schoennagel, T.: Spatiotemporal patterns of mountain pine
1039 beetle activity in the southern Rocky Mountains, *Ecology*, 93, 2175-2185, 2012.

1040 Chiang, F., Mazdiyasn, O., and AghaKouchak, A.: Evidence of anthropogenic impacts on global
1041 drought frequency, duration, and intensity, *Nat Commun.*, 12, 2754,
1042 <https://doi.org/10.1038/s41467-021-22314-w>, 2021.

1043 Choat, B., Brodribb, T.J., Brodersen, C.R., Duursma, R.A., López, R., and Medlyn, B.E.: Triggers
1044 of tree mortality under drought, *Nature*, 558, 531-539, 2018.

1045 Choat, B., Jansen, S., Brodribb, T.J., Cochard, H., Delzon, S., Bhaskar, R. et al.: Global
1046 convergence in the vulnerability of forests to drought, *Nature*, 491, 752-755, 2012.

1047 Christoffersen, B.O., Gloor, M., Fauset, S., Fyllas, N.M., Galbraith, D.R., Baker, T.R. et al.:
1048 Linking hydraulic traits to tropical forest function in a size-structured and trait-driven model
1049 (TFS v.1-Hydro), *Geosci. Model Dev. Discuss.*, 2016, 1-60, 2016.

1050 Ciais, P., Reichstein, M., Viovy, N., Granier, A., Ogée, J., Allard, V. et al.: Europe-wide
1051 reduction in primary productivity caused by the heat and drought in 2003, *Nature*, 437, 529,
1052 2005.

1053 Clark, K.L., Skowronski, N., and Hom, J.: Invasive insects impact forest carbon dynamics, *Glob.*
1054 *Change Biol.*, 16, 88-101, 2010.

1055 Coley, P., Massa, M., Lovelock, C., Winter, K.: Effects of elevated CO₂ on foliar chemistry of
1056 saplings of nine species of tropical tree, *Oecologia*, 2002.

1057 Creeden, E.P., Hicke, J.A., and Buotte, P.C.: Climate, weather, and recent mountain pine beetle
1058 outbreaks in the western United States, *Forest Ecol. Manag.*, 312, 239-251, 2014.

1059 D'Amato, A.W., Bradford, J.B., Fraver, S. and Palik, B.J.: Effects of thinning on drought
1060 vulnerability and climate response in north temperate forest ecosystems, *Eco. Applications*,
1061 23, 1735-1742, 2013.

1062 da Costa, A.C.L., Galbraith, D., Almeida, S., Portela, B.T.T., da Costa, M., de Athaydes Silva
1063 Junior, J. et al., Effect of 7 yr of experimental drought on vegetation dynamics and biomass
1064 storage of an eastern Amazonian rainforest, *New Phytol.*, 187, 579-591, 2010.

1065 De Kauwe, M.G., Medlyn, B.E., Zaehle, S., Walker, A.P., Dietze, M.C., Wang, Y.-P. et al.:
1066 Where does the carbon go? A model-data intercomparison of vegetation carbon allocation
1067 and turnover processes at two temperate forest free-air CO₂ enrichment sites, *New Phytol.*,
1068 203, 883-899, 2014.

1069 Dietze, M.C., and Matthes, J.H.: A general ecophysiological framework for modelling the impact
1070 of pests and pathogens on forest ecosystems, *Ecol. Lett.*, 17, 1418-1426, 2014.

1071 Döscher, R., Acosta, M., et al.: The EC-Earth3 Earth System Model for the Climate Model
1072 Intercomparison Project 6, *Geosci. Model Dev. Discuss.* [preprint],
1073 <https://doi.org/10.5194/gmd-2020-446>, in revision, 2022.

1074 Dreesen, F.E., De Boeck, H.J., Janssens, I.A., and Nijs, I.: Do successive climate extremes
1075 weaken the resistance of plant communities? An experimental study using plant
1076 assemblages, *Biogeosciences*, 11, 109-121, 2014.

1077 Eamus, D., Boulain, N., Cleverly, J., and Breshears, D.D.: Global change-type drought-induced
1078 tree mortality: vapor pressure deficit is more important than temperature per se in causing
1079 decline in tree health, *Ecol. Evol.*, 3, 2711-2729, 2013.

1080 Eller, C.B., Rowland, L., Mencuccini, M., Rosas, T., Williams, K., Harper, A. et al.: Stomatal
1081 optimization based on xylem hydraulics (SOX) improves land surface model simulation of
1082 vegetation responses to climate, *New Phytol.*, 226, 1622-
1083 1637, <https://doi.org/10.1111/nph.16419>, 2020.

1084 Ellsworth, David S., Anderson, Ian C., Crous, Kristine Y., Cooke, J., Drake, John E., Gherlenda,
1085 Andrew N. et al.: Elevated CO₂ does not increase eucalypt forest productivity on a low-
1086 phosphorus soil, *Nature Climate Change*, 7, 279, 2017.

1087 ENQUIST, B.J., and ENQUIST, C.A.F.: Long-term change within a Neotropical forest: assessing
1088 differential functional and floristic responses to disturbance and drought, *Glob. Change*
1089 *Biol.*, 17, 1408-1424, 2011.

1090 Esquivel-Muelbert, A., Baker, T.R., Dexter, K.G., Lewis, S.L., Brienen, R.J.W., Feldpausch, T.R.
1091 et al.: Compositional response of Amazon forests to climate change, *Glob. Change Biol.*, 25,
1092 39-56, 2019.

1093 Eziz, A., Yan, Z., Tian, D., Han, W., Tang, Z., and Fang, J.: Drought effect on plant biomass
1094 allocation: A meta-analysis, *Ecol. Evol.*, 7, 11002-11010, 2017.

1095 Fang, Y., Leung, L. R., Knox, R., Koven, C., and Bond-Lamberty, B.: Impact of the numerical
1096 solution approach of a plant hydrodynamic model (v0.1) on vegetation dynamics, *Geosci.*
1097 *Model Dev.*, 15, 6385–6398, <https://doi.org/10.5194/gmd-15-6385-2022>, 2022.

1098 Feldpausch, T.R., Phillips, O.L., Brienen, R.J.W., Gloor, E., Lloyd, J., Lopez-Gonzalez, G. et al.:
1099 Amazon forest response to repeated droughts, *Global Biogeochemical Cycles*, 30, 964-982,
1100 2016.

1101 Fisher, R.A., Muszala, S., Verstein, M., Lawrence, P., Xu, C., McDowell, N.G. et al.: Taking
1102 off the training wheels: the properties of a dynamic vegetation model without climate
1103 envelopes, *CLM4.5(ED)*, *Geosci. Model Dev.*, 8, 3593-3619, 2015.

1104 Fisher, R.A., Koven, C.D., Anderegg, W.R.L., Christoffersen, B.O., Dietze, M.C., Farrior, C.E. et
1105 al.: Vegetation demographics in Earth System Models: A review of progress and priorities,
1106 *Glob. Change Biol.*, 24, 35-54, 2018.

1107 Fisher, R. A., and Koven, C. D.: Perspectives on the future of land surface models and the
1108 challenges of representing complex terrestrial systems, *JAMES*, 12,
1109 e2018MS001453, <https://doi.org/10.1029/2018MS001453>, 2020.

1110 Fleischer, K., Rammig, A., De Kauwe, M.G., Walker, A.P., Domingues, T.F., Fuchslueger, L. et
1111 al.: Amazon forest response to CO₂ fertilization dependent on plant phosphorus acquisition,
1112 *Nature Geoscience*, 12, 736-741, 2019.

1113 Frank, D., Reichstein, M., Bahn, M., Thonicke, K., Frank, D., Mahecha, M.D. et al.: Effects of
1114 climate extremes on the terrestrial carbon cycle: concepts, processes and potential future
1115 impacts, *Glob. Change Biol.*, 21, 2861-2880, 2015.

1116 Franklin, O., McMurtrie, R.E., Iversen, C.M., Crous, K.Y., Finzi, A.C., Tissue, D.T., Ellsworth,
1117 D.S., Oren, R. Norby, R.J.: Forest fine-root production and nitrogen use under elevated
1118 CO₂: contrasting responses in evergreen and deciduous trees explained by a common
1119 principle, *Glob. Change Biol.*, 15, 132-144, 2009.

1120 Franklin, O., Johansson, J., Dewar, R.C., Dieckmann, U., McMurtrie, R.E., Brännström, Å.,
1121 Dybzinski, R.: Modeling carbon allocation in trees: a search for principles, *Tree Physiology*,
1122 32, 648–666, <https://doi.org/10.1093/treephys/tpr138>, 2012.

1123 Franklin, O., Harrison, S.P., Dewar, R. et al.: Organizing principles for vegetation dynamics. *Nat.*
1124 *Plants*, 6, 444–453, <https://doi.org/10.1038/s41477-020-0655-x>, 2020.

1125 Friend, A.D., Lucht, W., Rademacher, T.T., Keribin, R., Betts, R., Cadule, P. et al.: Carbon
1126 residence time dominates uncertainty in terrestrial vegetation responses to future climate
1127 and atmospheric CO₂, *PNAS*, 111, 3280-3285, 2014.

1128 Gerten, D., LUO, Y., Le MAIRE, G., PARTON, W.J., KEOUGH, C., WENG, E. et al.: Modelled
1129 effects of precipitation on ecosystem carbon and water dynamics in different climatic zones,
1130 *Glob. Change Biol.*, 14, 2365-2379, 2008.

1131 Goulden, M.L., and Bales, R.C.: California forest die-off linked to multi-year deep soil drying in
1132 2012–2015 drought, *Nature Geoscience*, 12, 632-637, 2019.

1133 Gray, S.B., Dermody, O., Klein, S.P., Locke, A.M., McGrath, J.M., Paul, R.E. et al.: Intensifying
1134 drought eliminates the expected benefits of elevated carbon dioxide for soybean, *Nature*
1135 *Plants*, 2, 16132, 2016.

1136 Greenwood, S., Ruiz-Benito, P., Martínez-Vilalta, J., Lloret, F., Kitzberger, T., Allen, C.D. et al.:
1137 Tree mortality across biomes is promoted by drought intensity, lower wood density and
1138 higher specific leaf area, *Ecol. Lett.*, 20, 539-553, 2017.

1139 Griffin, D., and Anchukaitis, K.J.: How unusual is the 2012–2014 California drought? *Geophys.*
1140 *Res. Lett.*, 41, 9017-9023, 2014.

1141 Hanbury-Brown, A.R., Powell, T.L., Muller-Landau, H.C., Wright, S.J. and Kueppers, L.M.:
1142 Simulating environmentally-sensitive tree recruitment in vegetation demographic models,
1143 *New Phytol.*, 235, 78-93, <https://doi.org/10.1111/nph.18059>, 2022.

1144 Harrison, S.P., Cramer, W., Franklin, O., Prentice, I.C., Wang, H., Brännström, Å., et al.: Eco-
1145 evolutionary optimality as a means to improve vegetation and land-surface models, *New*
1146 *Phytol.*, 231, 2125-2141, <https://doi.org/10.1111/nph.17558>, 2021.

1147 Hickler, T., Smith, B., Sykes, M.T., Davis, M.B., Sugita, S., and Walker, K.: USING A
1148 GENERALIZED VEGETATION MODEL TO SIMULATE VEGETATION DYNAMICS
1149 IN NORTHEASTERN USA, *Ecology*, 85, 519-530, 2004.

1150 Holm, J. A., Knox, R. G., Zhu, Q., Fisher, R. A., Koven, C. D., Nogueira Lima, A. J., et al.: The
1151 central Amazon biomass sink under current and future atmospheric CO₂: Predictions from
1152 big-leaf and demographic vegetation models, *J. Geophys. Res. Biogeosciences*, 125,
1153 e2019JG005500. <https://doi.org/10.1029/2019JG005500>, 2020.

1154 Hovenden, M.J., Newton, P.C.D., and Wills, K.E.: Seasonal not annual rainfall determines
1155 grassland biomass response to carbon dioxide, *Nature*, 511, 583, 2014.

1156 Hubbard, R.M., Rhoades, C.C., Elder, K., and Negron, J.: Changes in transpiration and foliage
1157 growth in lodgepole pine trees following mountain pine beetle attack and mechanical
1158 girdling, *Forest Ecol. Manag.*, 289, 312-317, 2013.

1159 IPCC: Managing the Risks of Extreme Events and Disasters to Advance Climate Change
1160 Adaptation. A Special Report of Working Groups I and II of the Intergovernmental Panel on
1161 Climate Change. (ed. Field, C.B., V. Barros, T.F. Stocker, D. Qin, D.J. Dokken, K.L. Ebi,
1162 M.D. Mastrandrea, K.J. Mach, G.-K. Plattner, S.K. Allen, M. Tignor, and P.M. Midgley)
1163 Cambridge, UK, and New York, NY, USA, p. 582 pp, 2012.

1164 IPCC: Climate Change 2021: The Physical Science Basis. Contribution of Working Group I to the
1165 Sixth Assessment Report of the Intergovernmental Panel on Climate Change [Masson-
1166 Delmotte, V., P. Zhai, A. Pirani, S.L. Connors, C. Péan, S. Berger, N. Caud, Y. Chen, L.
1167 Goldfarb, M.I. Gomis, M. Huang, K. Leitzell, E. Lonnoy, J.B.R. Matthews, T.K. Maycock,
1168 T. Waterfield, O. Yelekçi, R. Yu, and B. Zhou (eds.)]. Cambridge University Press, 2021.

1169 Jiang, M., Medlyn, B.E., Drake, J.E., Duursma, R.A., Anderson, I.C., Barton, C.V.M., Boer,
1170 M.B., Carrillo, Y., Castañeda-Gómez, L., Collins, L., et al.: The fate of carbon in a mature
1171 forest under carbon dioxide enrichment, *Nature*, 580, 227-231,
1172 <https://doi.org/10.1038/s41586-020-2128-9>, 2020.

1173 Joslin, J.D., Wolfe, M.H., and Hanson, P.J.: Effects of altered water regimes on forest root
1174 systems, *New Phytol.*, 147, 117-129, 2000.

1175 Jump, A.S., Ruiz-Benito, P., Greenwood, S., Allen, C.D., Kitzberger, T., Fensham, R. et al.:
1176 Structural overshoot of tree growth with climate variability and the global spectrum of
1177 drought-induced forest dieback, *Glob. Change Biol.*, 23, 3742-3757, 2017.

1178 Kalacska, M.E.R., Sánchez-Azofeifa, G.A., Calvo-Alvarado, J.C., Rivard, B. and Quesada, M.:
1179 Effects of Season and Successional Stage on Leaf Area Index and Spectral Vegetation
1180 Indices in Three Mesoamerican Tropical Dry Forests, *Biotropica*, 37, 486-
1181 496, <https://doi.org/10.1111/j.1744-7429.2005.00067.x>, 2005.

1182 Kannenberg, S.A., Schwalm, C.R. and Anderegg, W.R.L.: Ghosts of the past: how drought legacy
1183 effects shape forest functioning and carbon cycling, *Ecol. Lett.*, 23: 891-901,
1184 <https://doi.org/10.1111/ele.13485>, 2020.

1185 Kattge, J., DÍAZ, S., LAVOREL, S., PRENTICE, I.C., LEADLEY, P., BÖNISCH, G. et al.: TRY
1186 – a global database of plant traits, *Global Change Biol*, 17, 2905-2935, 2011.

1187 Kayler, Z.E., De Boeck, H.J., Fatichi, S., Grünzweig, J.M., Merbold, L., Beier, C. et al.:
1188 Experiments to confront the environmental extremes of climate change, *Front. Ecol.*
1189 *Environ.*, 13, 219-225, 2015.

1190 Keenan, T.F., Hollinger, D.Y., Bohrer, G., Dragoni, D., Munger, J.W., Schmid, H.P. et al.:
1191 Increase in forest water-use efficiency as atmospheric carbon dioxide concentrations rise,
1192 *Nature*, 499, 324-327, 2013.

1193 Kennedy, D., Swenson, S., Oleson, K. W., Lawrence, D. M., Fisher, R., Lola da Costa, A. C., and
1194 Gentine, P.: Implementing plant hydraulics in the Community Land Model, version 5,
1195 *JAMES*, 11, 485– 513, <https://doi.org/10.1029/2018MS001500>, 2019.

1196 Li, L., Yang, Z.-L., Matheny, A. M., Zheng, H., Swenson, S. C., Lawrence, D. M., et
1197 al.: Representation of plant hydraulics in the Noah-MP land surface model: Model
1198 development and multiscale evaluation, *JAMES*, 13,
1199 e2020MS002214, <https://doi.org/10.1029/2020MS002214>, 2021.

1200 Li, Q., Lu, X., Wang, Y., Huang, X., Cox, P. M., and Luo, Y.: Leaf area index identified as a
1201 major source of variability in modeled CO₂ fertilization, *Biogeosciences*, 15, 6909–6925,
1202 <https://doi.org/10.5194/bg-15-6909-2018>, 2018.

1203 Liu, Y., Parolari, A.J., Kumar, M., Huang, C.-W., Katul, G.G., and Porporato, A.: Increasing
1204 atmospheric humidity and CO₂ concentration alleviate forest mortality risk, *PNAS*, 114,
1205 9918-9923, 2017.

1206 Lloret, F., Escudero, A., Iriondo, J.M., Martínez-Vilalta, J., and Valladares, F.: Extreme climatic
1207 events and vegetation: the role of stabilizing processes, *Glob. Change Biol.*, 18, 797-805,
1208 2012.

1209 Luo, Y., Gerten, D., Le Maire, G., Parton, W.J., Weng, E., Zhou, X. et al.: Modeled interactive
1210 effects of precipitation, temperature, and [CO₂] on ecosystem carbon and water dynamics in
1211 different climatic zones, *Glob. Change Biol.*, 14, 1986-1999, 2008.

1212 Luo, Y.Q., Randerson, J.T., Abramowitz, G., Bacour, C., Blyth, E., Carvalhais, N. et al.: A
1213 framework for benchmarking land models, *Biogeosciences*, 9, 3857-3874, 2012.

1214 Luo, Y., Jiang, L., Niu, S., Zhou, X.: Nonlinear responses of land ecosystems to variation in
1215 precipitation, *New Phytol.*, 214, 5–7, 2017.

1216 Ma, W., Zhai, L., Pivovarov, A., Shuman, J., Buotte, P., Ding, J., Christoffersen, B., Knox, R.,
1217 Moritz, M., Fisher, R. A., Koven, C. D., Kueppers, L., and Xu, C.: Assessing climate

1218 change impacts on live fuel moisture and wildfire risk using a hydrodynamic vegetation
1219 model, *Biogeosciences*, 18, 4005–4020, <https://doi.org/10.5194/bg-18-4005-2021>, 2021.

1220 MacGillivray, C.W., Grime, J.P., and The Integrated Screening Programme, T.: Testing
1221 Predictions of the Resistance and Resilience of Vegetation Subjected to Extreme Events,
1222 *Funct. Ecol.*, 9, 640-649, 1995.

1223 Markewitz, D., Devine, S., Davidson, E.A., Brando, P., and Nepstad, D.C.: Soil moisture
1224 depletion under simulated drought in the Amazon: impacts on deep root uptake, *New*
1225 *Phytol.*, 187, 592-607, 2010.

1226 Matusick, G., Ruthrof, K.X., Brouwers, N.C., Dell, B., and Hardy, G.S.J.: Sudden forest canopy
1227 collapse corresponding with extreme drought and heat in a mediterranean-type eucalypt
1228 forest in southwestern Australia, *European J. Forest Res.*, 132, 497-510, 2013.

1229 Matusick, G., Ruthrof, K.X., Fontaine, J.B., and Hardy, G.E.S.J.: Eucalyptus forest shows low
1230 structural resistance and resilience to climate change-type drought, *J. Vegetation Science*,
1231 27, 493-503, 2016.

1232 McCarthy, M.C., and Enquist, B.J.: Consistency between an allometric approach and optimal
1233 partitioning theory in global patterns of plant biomass allocation, *Funct. Ecol.*, 21, 713-720,
1234 2007.

1235 McDowell, N., Pockman, W.T., Allen, C.D., Breshears, D.D., Cobb, N., Kolb, T. et al.:
1236 Mechanisms of plant survival and mortality during drought: why do some plants survive
1237 while others succumb to drought? *New Phytol.*, 178, 719-739, 2008.

1238 McDowell, N.G., Adams, H.D., Bailey, J.D., Hess, M., and Kolb, T.E.: Homeostatic Maintenance
1239 Of Ponderosa Pine Gas Exchange In Response To Stand Density Changes, *Ecological*
1240 *Applications*, 16, 1164-1182, 2006.

1241 McDowell, N.G., and Allen, C.D.: Darcy's law predicts widespread forest mortality under climate
1242 warming, *Nature Climate Change*, 5, 669-672, 2015.

1243 McDowell, N.G., Beerling, D.J., Breshears, D.D., Fisher, R.A., Raffa, K.F., and Stitt, M.: The
1244 interdependence of mechanisms underlying climate-driven vegetation mortality, *Trends in*
1245 *Ecol. & Evolution*, 26, 523-532, 2011.

1246 McDowell, N.G., Fisher, R.A., Xu, C., Domec, J.C., Hölttä, T., Mackay, D.S. et al.: Evaluating
1247 theories of drought-induced vegetation mortality using a multimodel–experiment
1248 framework, *New Phytol.*, 200, 304-321, 2013.

1249 Medlyn, B.E., De Kauwe, M.G., Zaehle, S., Walker, A.P., Duursma, R.A., Luus, K., Mishurov,
1250 M., Pak, B., Smith, B., Wang, Y.-P., Yang, X., Crous, K.Y., Drake, J.E., Gimeno, T.E.,
1251 Macdonald, C.A., Norby, R.J., Power, S.A., Tjoelker, M.G. and Ellsworth, D.S.: Using
1252 models to guide field experiments: a priori predictions for the CO₂ response of a nutrient-
1253 and water-limited native Eucalypt woodland, *Glob. Change Biol.*, 22, 2834-2851, 2016.

1254 Medvigy, D., Wang, G., Zhu, Q., Riley, W.J., Trierweiler, A.M., Waring, B., Xu, X. and Powers,
1255 J.S.: Observed variation in soil properties can drive large variation in modelled forest
1256 functioning and composition during tropical forest secondary succession, *New Phytol*, 223,
1257 1820-1833, <https://doi.org/10.1111/nph.15848>, 2019.

1258 Medvigy, D., Clark, K.L., Skowronski, N.S., and Schäfer, K.V.R.: Simulated impacts of insect
1259 defoliation on forest carbon dynamics, *Environ. Res. Lett.*, 7, 045703, 2012.

1260 Medvigy, D. and Moorcroft, P.R.: Predicting ecosystem dynamics at regional scales: an
1261 evaluation of a terrestrial biosphere model for the forests of northeastern North America,
1262 *Philosophical Transactions of the Royal Society B: Biological Sciences*, 367, 222-235,
1263 2012.

1264 Medvigy, D., Wofsy, S., Munger, J., Hollinger, D. and Moorcroft, P.: Mechanistic scaling of
1265 ecosystem function and dynamics in space and time: Ecosystem Demography model version
1266 2, *J. Geophys. Res. Biogeosciences*, 114, 2009.

1267 Mencuccini, M., Manzoni, S., and Christoffersen, B.: Modelling water fluxes in plants: from
1268 tissues to biosphere, *New Phytol.*, 222, 1207-1222, <https://doi.org/10.1111/nph.15681>, 2019.

1269 Meir, P., Wood, T.E., Galbraith, D.R., Brando, P.M., Da Costa, A.C.L., Rowland, L. et al.:
1270 Threshold Responses to Soil Moisture Deficit by Trees and Soil in Tropical Rain Forests:
1271 Insights from Field Experiments, *BioScience*, 65, 882-892, 2015.

1272 Montané, F., Fox, A.M., Arellano, A.F., MacBean, N., Alexander, M.R., Dye, A. et al.:
1273 Evaluating the effect of alternative carbon allocation schemes in a land surface model
1274 (CLM4.5) on carbon fluxes, pools, and turnover in temperate forests, *Geosci. Model Dev.*,
1275 10, 3499-3517, 2017.

1276 Muldavin, E.H., Moore, D.I., Collins, S.L., Wetherill, K.R., and Lightfoot, D.C.: Aboveground
1277 net primary production dynamics in a northern Chihuahuan Desert ecosystem, *Oecologia*,
1278 155, 123-132, 2008.

1279 Myers, J.A., and Kitajima, K.: Carbohydrate storage enhances seedling shade and stress tolerance
1280 in a neotropical forest, *J. Ecology*, 95, 383-395, 2007.

1281 Niklas, K. J.: The scaling of plant height: A comparison among major plant clades and anatomical
1282 grades, *Annals of Botany*, 72, 165–172, <https://doi.org/10.1006/anbo.1993.1095>, 1993.

1283 Norby, R.J., DeLucia, E.H., Gielen, B., Calfapietra, C., Giardina, C.P., King, J.S. et al.: Forest
1284 response to elevated CO₂ is conserved across a broad range of productivity, *PNAS*, 102,
1285 18052-18056, 2005.

1286 O'Brien, M.J., Leuzinger, S., Philipson, C.D., Tay, J., and Hector, A.: Drought survival of
1287 tropical tree seedlings enhanced by non-structural carbohydrate levels, *Nature Climate
1288 Change*, 4, 710, 2014.

1289 Obermeier, W.A., Lehnert, L.W., Kammann, C.I., Müller, C., Grünhage, L., Luterbacher, J. et al.:
1290 Reduced CO₂ fertilization effect in temperate C₃ grasslands under more extreme weather
1291 conditions, *Nature Climate Change*, 7, 137, 2016.

1292 Palace, M., Keller, M., and Silva, H.: NECROMASS PRODUCTION: STUDIES IN
1293 UNDISTURBED AND LOGGED AMAZON FORESTS, *Ecological Applications*, 18, 873-
1294 884, 2008.

1295 Petit, G., Anfodillo, T., Mencuccini, M.: Tapering of xylem conduits and hydraulic limitations in
1296 sycamore (*Acer pseudoplatanus*) trees, *New Phytol.*, 177, 653-
1297 664. <https://doi.org/10.1111/j.1469-8137.2007.02291.x>, 2008.

1298 Phillips, O.L., Aragão, L.E.O.C., Lewis, S.L., Fisher, J.B., Lloyd, J., López-González, G. et al.:
1299 Drought Sensitivity of the Amazon Rainforest, *Science*, 323, 1344-1347, 2009.

1300 Phillips, O.L., van der Heijden, G., Lewis, S.L., López-González, G., Aragão, L.E.O.C., Lloyd, J.
1301 et al.: Drought–mortality relationships for tropical forests, *New Phytol.*, 187, 631-646, 2010.

1302 Pilon, C.E., Côté, B., and Fyles, J.W.: Effect of an artificially induced drought on leaf peroxidase
1303 activity, mineral nutrition and growth of sugar maple, *Plant and Soil*, 179, 151-158, 1996.

1304 Potter, C., Klooster, S., Hiatt, C., Genovese, V., and Castilla-Rubio, J.C.: Changes in the carbon
1305 cycle of Amazon ecosystems during the 2010 drought, *Environ. Res. Lett.*, 6, 034024, 2011.

1306 Powell, T.L., Galbraith, D.R., Christoffersen, B.O., Harper, A., Imbuzeiro, H.M.A., Rowland, L.
1307 et al.: Confronting model predictions of carbon fluxes with measurements of Amazon
1308 forests subjected to experimental drought, *New Phytol.*, 200, 350-365, 2013.

- 1309 Powell, T.L., Koven, C.D., Johnson, D.J., Faybishenko, B., Fisher, R.A., Knox, Ryan G. et al.:
 1310 Variation in hydroclimate sustains tropical forest biomass and promotes functional diversity,
 1311 *New Phytol.*, 219, 932-946, 2018.
- 1312 Powers, J.S., Becknell, J.M., Irving, J., and Pérez-Aviles, D.: Diversity and structure of
 1313 regenerating tropical dry forests in Costa Rica: Geographic patterns and environmental
 1314 drivers, *Forest Ecol. Manag.*, 258, 959-970, 2009.
- 1315 Powers, J.S., and Pérez-Aviles, D.: Edaphic Factors are a More Important Control on Surface
 1316 Fine Roots than Stand Age in Secondary Tropical Dry Forests, *Biotropica*, 45, 1-9, 2013.
- 1317 Powers, JS, Vargas G., G, Brodribb, TJ, et al.: A catastrophic tropical drought kills hydraulically
 1318 vulnerable tree species, *Glob. Change Biol.* 2020; 26: 3122– 3133,
 1319 <https://doi.org/10.1111/gcb.15037>, 2020.
- 1320 Pugh, T.A.M., Rademacher, T., Shafer, S. L., Steinkamp, J., Barichivich, J., Beckage, B. et al.:
 1321 Understanding the uncertainty in global forest carbon turnover, *Biogeosciences*, 17, 3961–
 1322 3989, <https://doi.org/10.5194/bg-17-3961-2020>, 2020.
- 1323 Rapparini, F., and Peñuelas, J.: Mycorrhizal Fungi to Alleviate Drought Stress on Plant Growth.
 1324 In: *Use of Microbes for the Alleviation of Soil Stresses*, Volume 1 (ed. Miransari, M),
 1325 Springer New York New York, NY, pp. 21-42, 2014.
- 1326 Reich, P.B., Hobbie, S.E., and Lee, T.D.: Plant growth enhancement by elevated CO₂ eliminated
 1327 by joint water and nitrogen limitation, *Nature Geoscience*, 7, 920, 2014.
- 1328 Reich, P.B., Wright, I.J., and Lusk, C.H.: PREDICTING LEAF PHYSIOLOGY FROM SIMPLE
 1329 PLANT AND CLIMATE ATTRIBUTES: A GLOBAL GLOPNET ANALYSIS, *Ecological*
 1330 *Applications*, 17, 1982-1988, 2007.
- 1331 Reichstein, M., Bahn, M., Ciais, P., Frank, D., Mahecha, M.D., Seneviratne, S.I. et al.: Climate
 1332 extremes and the carbon cycle, *Nature*, 500, 287-295, 2013.
- 1333 Reyes, J.J., Tague, C.L., Evans, R.D., and Adam, J.C.: Assessing the Impact of Parameter
 1334 Uncertainty on Modeling Grass Biomass Using a Hybrid Carbon Allocation Strategy, 9,
 1335 2968-2992, 2017.
- 1336 Richardson, A.D., Carbone, M.S., Keenan, T.F., Czimczik, C.I., Hollinger, D.Y., Murakami, P. et
 1337 al.: Seasonal dynamics and age of stemwood nonstructural carbohydrates in temperate forest
 1338 trees, *New Phytol.*, 197, 850-861, 2013.
- 1339 Rowland, L., da Costa, A.C.L., Galbraith, D.R., Oliveira, R.S., Binks, O.J., Oliveira, A.A.R. et
 1340 al.: Death from drought in tropical forests is triggered by hydraulics not carbon starvation,
 1341 *Nature*, 528, 119, 2015.
- 1342 Roy, J., Picon-Cochard, C., Augusti, A., Benot, M.-L., Thiery, L., Darsonville, O. et al.: Elevated
 1343 CO₂ maintains grassland net carbon uptake under a future heat and drought extreme, *PNAS*,
 1344 113, 6224-6229, 2016.
- 1345 Ruppert, J.C., Harmony, K., Henkin, Z., Snyman, H.A., Sternberg, M., Willms, W. et al.:
 1346 Quantifying drylands' drought resistance and recovery: the importance of drought intensity,
 1347 dominant life history and grazing regime, *Glob. Change Biol.*, 21, 1258-1270, 2015.
- 1348 Rustad, L.E.: The response of terrestrial ecosystems to global climate change: Towards an
 1349 integrated approach, *Science of The Total Environ.*, 404, 222-235, 2008.
- 1350 Ruthrof, K.X., Breshears, D.D., Fontaine, J.B., Froend, R.H., Matusick, G., Kala, J. et al.:
 1351 Subcontinental heat wave triggers terrestrial and marine, multi-taxa responses, *Scientific*
 1352 *Reports*, 8, 13094, 2018.
- 1353 Scheiter, S., Langan, L., and Higgins, S.I.: Next-generation dynamic global vegetation models:
 1354 learning from community ecology, *New Phytol.*, 198, 957-969, 2013.

1355 Schenk, H.J., and Jackson, R.B.: Mapping the global distribution of deep roots in relation to
1356 climate and soil characteristics, *Geoderma*, 126, 129-140, 2005.

1357 Schwalm, C.R., Anderegg, W.R.L., Michalak, A.M., Fisher, J.B., Biondi, F., Koch, G. et al.:
1358 Global patterns of drought recovery, *Nature*, 548, 202, 2017.

1359 Seneviratne, S.I., X. Zhang, M. Adnan, W. Badi, C. Dereczynski, A. Di Luca, S. Ghosh, I.
1360 Iskandar, J. Kossin, S. Lewis, F. Otto, I. Pinto, M. Satoh, S.M. Vicente-Serrano, M. Wehner,
1361 and B. Zhou, 2021: Weather and Climate Extreme Events in a Changing Climate. In
1362 *Climate Change 2021: The Physical Science Basis. Contribution of Working Group I to the*
1363 *Sixth Assessment Report of the Intergovernmental Panel on Climate Change* [Masson-
1364 Delmotte, V., P. Zhai, A. Pirani, S.L. Connors, C. Péan, S. Berger, N. Caud, Y. Chen, L.
1365 Goldfarb, M.I. Gomis, M. Huang, K. Leitzell, E. Lonnoy, J.B.R. Matthews, T.K. Maycock,
1366 T. Waterfield, O. Yelekçi, R. Yu, and B. Zhou (eds.)], Cambridge University Press,
1367 Cambridge, United Kingdom and New York, NY, USA, pp. 1513–1766,
1368 doi:10.1017/9781009157896.013, 2021.

1369 Settele, J., Scholes, R., Betts, R., Bunn, S.E., Leadley, P., Nepstad, D., Overpeck, J.T., and
1370 Taboada, M.A.: Terrestrial and inland water systems. In: *Climate Change 2014: Impacts,*
1371 *Adaptation, and Vulnerability. Part A: Global and Sectoral Aspects. Contribution of*
1372 *Working Group II to the Fifth Assessment Report of the Intergovernmental Panel on*
1373 *Climate Change*, Cambridge University Press Cambridge, United Kingdom and New York,
1374 NY, USA, pp. 271-359, 2014.

1375 Sheffield, J., Goteti, G., and Wood, E.F.: Development of a 50-Year High-Resolution Global
1376 Dataset of Meteorological Forcings for Land Surface Modeling, *J. Climate*, 19, 3088-3111,
1377 2006.

1378 Shiels, A.B., Zimmerman, J.K., García-Montiel, D.C., Jonckheere, I., Holm, J., Horton, D. et al.:
1379 Plant responses to simulated hurricane impacts in a subtropical wet forest, Puerto Rico, *J.*
1380 *Ecology*, 98, 659-673, 2010.

1381 Silva, M., Matheny, A. M., Pauwels, V. R. N., Triadis, D., Missik, J. E., Bohrer, G., and Daly, E.:
1382 Tree hydrodynamic modelling of the soil–plant–atmosphere continuum using FETCH3,
1383 *Geosci. Model Dev.*, 15, 2619–2634, <https://doi.org/10.5194/gmd-15-2619-2022>, 2022.

1384 Sippel, S., Zscheischler, J., and Reichstein, M.: Ecosystem impacts of climate extremes crucially
1385 depend on the timing, *PNAS*, 113, 5768-5770, 2016.

1386 Sitch, S., HUNTINGFORD, C., GEDNEY, N., LEVY, P.E., LOMAS, M., PIAO, S.L. et al.:
1387 Evaluation of the terrestrial carbon cycle, future plant geography and climate-carbon cycle
1388 feedbacks using five Dynamic Global Vegetation Models (DGVMs), *Glob. Change Biol.*,
1389 14, 2015-2039, 2008.

1390 Skelton, R.P., West, A.G., and Dawson, T.E.: Predicting plant vulnerability to drought in
1391 biodiverse regions using functional traits, *PNAS*, 112, 5744-5749, 2015.

1392 Smith, B., Prentice, I.C., and Sykes, M.T.: Representation of vegetation dynamics in the
1393 modelling of terrestrial ecosystems: comparing two contrasting approaches within European
1394 climate space, *Global Ecol. Biogeo.*, 10, 621-637, 2001.

1395 Smith, B., Wårlind, D., Arneth, A., Hickler, T., Leadley, P., Siltberg, J. et al.: Implications of
1396 incorporating N cycling and N limitations on primary production in an individual-based
1397 dynamic vegetation model, *Biogeosciences*, 11, 2027-2054, 2014.

1398 Spasojevic, M.J., Bahlai, C.A., Bradley, B.A., Butterfield, B.J., Tuanmu, M.-N., Sistla, S. et al.:
1399 Scaling up the diversity–resilience relationship with trait databases and remote sensing data:
1400 the recovery of productivity after wildfire, *Glob. Change Biol.*, 22, 1421-1432, 2016.

1401 Sperry, J.S., Hacke, U.G., Oren, R., and Comstock, J.P.: Water deficits and hydraulic limits to
1402 leaf water supply, *Plant, Cell & Environ.*, 25, 251-263, 2002.

1403 Sperry, J.S., and Love, D.M.: What plant hydraulics can tell us about responses to climate-change
1404 droughts, *New Phytol.*, 207, 14-27, 2015.

1405 Sperry, J.S., Wang, Y., Wolfe, B.T., Mackay, D.S., Anderegg, W.R.L., McDowell, N.G. et al.:
1406 Pragmatic hydraulic theory predicts stomatal responses to climatic water deficits, *New*
1407 *Phytol.*, 212, 577-589, 2016.

1408 Stovall, A.E.L., Shugart, H., and Yang, X.: Tree height explains mortality risk during an intense
1409 drought, *Nature Communications*, 10, 4385, 2019.

1410 Tague, C.L., and Moritz, M.A.: Plant Accessible Water Storage Capacity and Tree-Scale Root
1411 Interactions Determine How Forest Density Reductions Alter Forest Water Use and
1412 Productivity, *Front. Forests and Global Change*, 2, 2019.

1413 Tomasella M, Petrusa E, Petruzzellis F, Nardini A, Casolo V.: The Possible Role of Non-
1414 Structural Carbohydrates in the Regulation of Tree Hydraulics, *International Journal of*
1415 *Molecular Sciences*, 21:144, <https://doi.org/10.3390/ijms21010144>, 2020.

1416 Trugman, A.T., Detto, M., Bartlett, M.K., Medvigy, D., Anderegg, W.R.L., Schwalm, C. et al.:
1417 Tree carbon allocation explains forest drought-kill and recovery patterns, *Ecol. Lett.*, 21,
1418 1552-1560, 2018.

1419 Trugman, A.T., Anderegg, L.D.L., Sperry, J.S., Wang, Y., Venturas, M., Anderegg,
1420 W.R.L.: Leveraging plant hydraulics to yield predictive and dynamic plant leaf allocation in
1421 vegetation models with climate change, *Glob. Change*
1422 *Biol.*, 25, 4008– 4021. <https://doi.org/10.1111/gcb.14814>, 2019.

1423 Uriarte, M., Lasky, J.R., Boukili, V.K., and Chazdon, R.L.: A trait-mediated, neighbourhood
1424 approach to quantify climate impacts on successional dynamics of tropical rainforests,
1425 *Funct. Ecol.*, 30, 157-167, 2016.

1426 Vargas G., G., Brodribb, T.J., Dupuy, J.M., González-M., R., Hulshof, C.M., Medvigy, D.,
1427 Allerton, T.A.P., Pizano, C., Salgado-Negret, B., Schwartz, N.B., Van Bloem, S.J., Waring,
1428 B.G. and Powers, J.S.: Beyond leaf habit: generalities in plant function across 97 tropical
1429 dry forest tree species, *New Phytol*, 232: 148-161. <https://doi.org/10.1111/nph.17584>, 2021.

1430 Venturas, M. D., Todd, H. N., Trugman, A. T., and Anderegg, W. R.: Understanding and
1431 predicting forest mortality in the western United States using long-term forest inventory data
1432 and modeled hydraulic damage, *New Phytol.*, 230, 1896-1910, 2021.

1433 Wang, D., Heckathorn, S.A., Wang, X., and Philpott, S.M.: A meta-analysis of plant
1434 physiological and growth responses to temperature and elevated CO₂, *Oecologia*, 169, 1-13,
1435 2012.

1436 Weng, E.S., Malyshev, S., Lichstein, J.W., Farrior, C.E., Dybzinski, R., Zhang, T. et al.: Scaling
1437 from individual trees to forests in an Earth system modeling framework using a
1438 mathematically tractable model of height-structured competition, *Biogeosciences*, 12, 2655-
1439 2694, 2015.

1440 Williams, A.P., Allen, C.D., Macalady, A.K., Griffin, D., Woodhouse, C.A., Meko, D.M. et al.:
1441 Temperature as a potent driver of regional forest drought stress and tree mortality, *Nature*
1442 *Climate Change*, 3, 292, 2012.

1443 Williams, A.P., Seager, R., Berkelhammer, M., Macalady, A.K., Crimmins, M.A., Swetnam,
1444 T.W. et al.: Causes and Implications of Extreme Atmospheric Moisture Demand during the
1445 Record-Breaking 2011 Wildfire Season in the Southwestern United States, *J. Applied*
1446 *Meteorology and Climatology*, 53, 2671-2684, 2014.

- 1447 Williams, L.J., Bunyavejchewin, S., and Baker, P.J.: Deciduousness in a seasonal tropical forest
1448 in western Thailand: interannual and intraspecific variation in timing, duration and
1449 environmental cues, *Oecologia*, 155, 571-582, 2008.
- 1450 Wullschleger, S.D., Hanson, P.J., and Todd, D.E.: Transpiration from a multi-species deciduous
1451 forest as estimated by xylem sap flow techniques, *For. Ecol. and Manage.*, 143, 205-213,
1452 2001.
- 1453 Xu, X., Medvigy, D., Powers, J.S., Becknell, J.M. and Guan, K.: Diversity in plant hydraulic
1454 traits explains seasonal and inter-annual variations of vegetation dynamics in seasonally dry
1455 tropical forests, *New Phytol.*, 212, 80-95, 2016.
- 1456 Yang, Y., Hillebrand, H., Lagisz, M., Cleasby, I., and Nakagawa, S.: Low statistical power and
1457 overestimated anthropogenic impacts, exacerbated by publication bias, dominate field
1458 studies in global change biology. *Glob. Change Biol.*, 28, 969– 989,
1459 <https://doi.org/10.1111/gcb.15972>, 2022.
- 1460 Zhu, K., Chiariello, N.R., Tobeck, T., Fukami, T., and Field, C.B.: Nonlinear, interacting
1461 responses to climate limit grassland production under global change, *PNAS*, 113, 10589-
1462 10594, 2016.
- 1463 Zhu, S-D., Chen, Y-J., Ye, Q., He, P-C., Liu, H., and Li, R-H., et al.: Leaf turgor loss point is
1464 correlated with drought tolerance and leaf carbon economics traits, *Tree Physiol.*, 38, 658–
1465 663, <https://doi.org/10.1093/treephys/tpy013>, 2018.
- 1466 Zscheischler, J., Mahecha, M.D., von Buttlar, J., Harmeling, S., Jung, M., Rammig, A. et al.: A
1467 few extreme events dominate global interannual variability in gross primary production,
1468 *Environ. Res. Lett.*, 9, 035001, 2014.